Report

Cell Reports

Synthetic Oligonucleotides Inhibit CRISPR-Cpf1-Mediated Genome Editing

Graphical Abstract

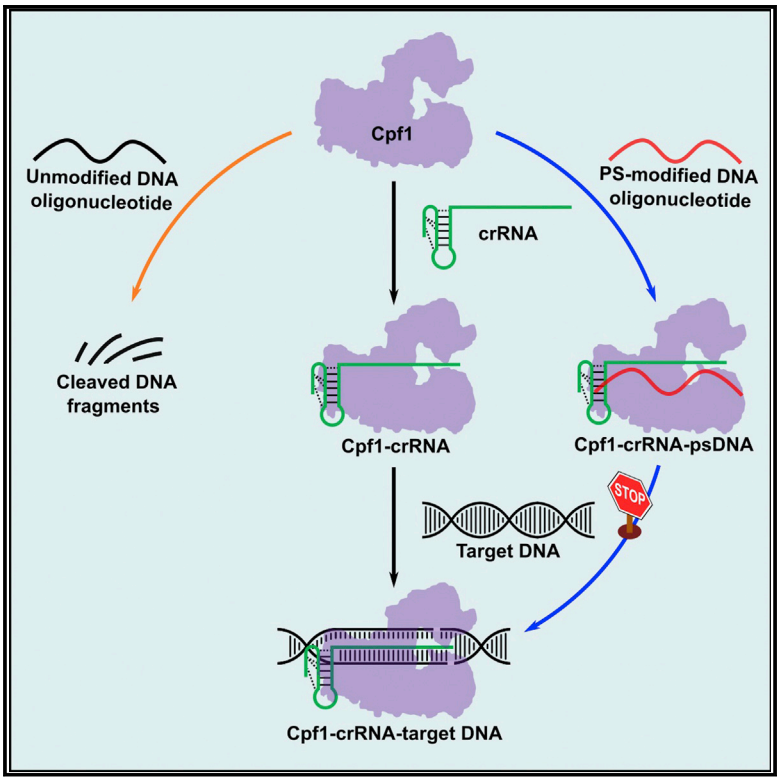

Authors

Bin Li, Chunxi Zeng, Wenqing Li, ..., Weiyu Zhao, Chengxiang Zhang, Yizhou Dong

Correspondence

dong.525@osu.edu

In Brief

Li et al. show that phosphorothioate-modified DNA (psDNA) oligonucleotides inhibit Cpf1-mediated genome-editing activity in a sequence-independent manner in human cells. These psDNA oligonucleotides interact with Cpf1 protein and block the formation of Cpf1-crRNA-target DNA complex. They also display inhibitory effects on the CRISPR-Cas9 system.

Highlights

- Phosphorothioate-modified DNA oligonucleotides inhibit Cpf1-mediated genome editing
- Inhibition of Cpf1 activity is time and dose dependent and target sequence independent
- psDNA oligonucleotides may block the complex formation of Cpf1-crRNA-DNA
- psDNA oligonucleotides inhibit Cas9-mediated genome editing

Li et al., 2018, Cell Reports *25*, 3262–3272
December 18, 2018
https://doi.org/10.1016/j.celrep.2018.11.079

CellPress

OPEN ACCESS
CellPress

Cell Reports
Report

Synthetic Oligonucleotides Inhibit CRISPR-Cpf1-Mediated Genome Editing

Bin Li,[1] Chunxi Zeng,[1] Wenqing Li,[1] Xinfu Zhang,[1] Xiao Luo,[1] Weiyu Zhao,[1] Chengxiang Zhang,[1] and Yizhou Dong[1,2,3,4,5,6,7,*]

[1]Division of Pharmaceutics and Pharmaceutical Chemistry, College of Pharmacy, The Ohio State University, Columbus, OH 43210, USA
[2]Department of Biomedical Engineering, The Ohio State University, Columbus, OH 43210, USA
[3]The Center for Clinical and Translational Science, The Ohio State University, Columbus, OH 43210, USA
[4]James Comprehensive Cancer Center, The Ohio State University, Columbus, OH 43210, USA
[5]Dorothy M. Davis Heart & Lung Research Institute, The Ohio State University, Columbus, OH 43210, USA
[6]Department of Radiation Oncology, The Ohio State University, Columbus, OH 43210, USA
[7]Lead Contact
*Correspondence: dong.525@osu.edu
https://doi.org/10.1016/j.celrep.2018.11.079

SUMMARY

Previously, researchers discovered a series of anti-CRISPR proteins that inhibit CRISPR-Cas activity, such as Cas9 and Cpf1 (Cas12a). Herein, we constructed crRNA variants consisting of chemically modified DNA-crRNA and RNA-crRNA duplexes and identified that phosphorothioate (PS)-modified DNA-crRNA duplex completely blocked the function of Cpf1. More important, without prehybridization, these PS-modified DNA oligonucleotides showed the ability to suppress DNA double-strand breaks induced by two Cpf1 orthologs, AsCpf1 and LbCpf1. Time-dependent inhibitory effects were validated in multiple loci of different human cells. Further studies demonstrated that PS-modified DNA oligonucleotides were able to serve as Cpf1 inhibitors in a sequence-independent manner. Mechanistic studies indicate that PS-modified DNA oligonucleotides hinder target DNA binding and recognition by Cpf1. Consequently, these synthetic DNA molecules expand the sources of CRISPR inhibitors, providing a platform to inactivate Cpf1-mediated genome editing.

INTRODUCTION

Cpf1 (CRISPR from *Prevotella* and *Francisella* 1, also known as Cas12a) is one of the bacterial endonucleases that can induce DNA double-strand breaks under the guidance of a single CRISPR RNA (crRNA) (Zetsche et al., 2015). Among the Cpf1 orthologs, AsCpf1 (Cpf1 from *Acidaminococcus sp.*) and LbCpf1 (Cpf1 from *Lachnospiraceae bacterium*) were reported for genome editing in human cells (Zetsche et al., 2015). The wild-type crRNA of CRISPR-Cpf1 system comprises a 5′ handle engaging Cpf1 recognition and a guide segment interacting with target DNA sequences through base-pairing (Dong et al., 2016; Fonfara et al., 2016; Yamano et al., 2016; Zetsche et al., 2015). Crystal structure of the Cpf1-crRNA-dsDNA complex uncovers the T-rich PAM recognition and cleavage mechanism by Cpf1 (Dong et al., 2016; Gao et al., 2016; Stella et al., 2017; Swarts et al., 2017; Yamano et al., 2016). On the basis of its unique genome-editing properties, the CRISPR-Cpf1 system has recently been applied in diverse eukaryotic species, including plants and animals, to achieve genome editing and base editing (Endo et al., 2016; Hur et al., 2016; Kim et al., 2016b, 2017; Li et al., 2018b; Tang et al., 2017; Wang et al., 2017; Xu et al., 2017; Zetsche et al., 2017; Zhang et al., 2017).

Although the CRISPR system offers a powerful platform for genome editing, a number of challenges exist for its therapeutic applications, including genome-editing efficiency and potential side effects (Bosley et al., 2015). To overcome these obstacles, extensive efforts have been made to improve genome-editing efficiency (Bin Moon et al., 2018; Dang et al., 2015; Hendel et al., 2015; Latorre et al., 2016; Li et al., 2017, 2018a; Lin et al., 2018; Park et al., 2018; Yamano et al., 2016; Ye et al., 2018). On the other hand, researchers investigated numerous approaches to modulate the activity of the CRISPR system. For example, stimuli responsive strategies such as chemical-, temperature-, and light-controlled approaches were developed to trigger or regulate the CRISPR-Cas system (Chow et al., 2018; DeLorenzo et al., 2018; Lee et al., 2016; Moreno-Mateos et al., 2017; Nuñez et al., 2016; Richter et al., 2017). Recently, anti-CRISPR (Acr) proteins from bacteriophages or bacteria were discovered to inhibit the function of type I, type II, and type V CRISPR-Cas systems (Borges et al., 2017; Dong et al., 2017; Harrington et al., 2017; Hynes et al., 2017, 2018; Landsberger et al., 2018; Marino et al., 2018; Maxwell, 2017; Pawluk et al., 2016a, 2016b; Rauch et al., 2017; Shin et al., 2017; Watters et al., 2018; Yang and Patel, 2017). These findings provide a potential approach to switch off the endonuclease activity of CRISPR-Cas when severe side effects occur in therapeutic applications in the future. Currently, no synthetic inhibitor has been reported for the CRISPR-Cas system. In this study, we investigated an array of crRNA duplexes (crDuplex) formed by hybridization of crRNA with DNA or RNA oligonucleotides and identified that DNA oligonucleotides bearing phosphorothioate (PS) linkages were capable of abolishing the cleavage activity of CRISPR-Cpf1 system in a sequence-independent manner. Similar inhibition effects were also observed in the CRISPR-Cas9 system.

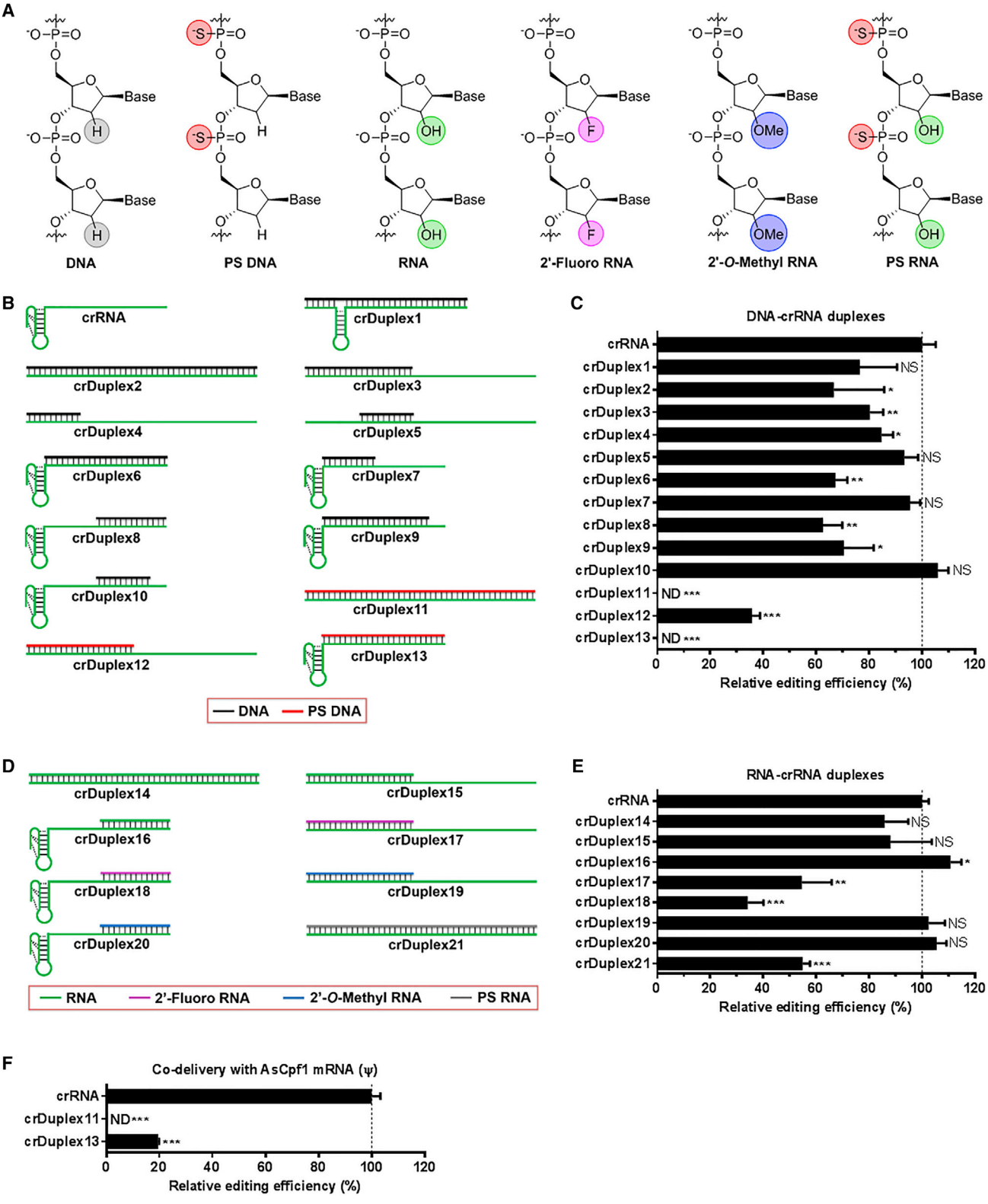

(legend on next page)

RESULTS

Effects of crDuplex on Cpf1-Mediated Genome Editing

Oligonucleotides are short single-stranded DNA or RNA molecules that have been widely used for diverse applications (Juliano, 2016; Wan and Seth, 2016). Previously, chemically modified nucleotides were extensively applied to tune the properties of oligonucleotides, such chemical stability and binding affinity (Deleavey and Damha, 2012; Hendel et al., 2015; Juliano, 2016; Lee et al., 2017; Li et al., 2016; Wan and Seth, 2016; Watts et al., 2008). Given the crucial role of crRNA in the formation of Cpf1-crRNA-DNA complex, we hypothesized that an oligonucleotide complementary to crRNA may provide a strategy to regulate Cpf1-mediated genome editing. To test this hypothesis, we designed a series of oligonucleotides using unmodified and chemically modified nucleotides (Figure 1A; Table S1). Because the crRNA of Cpf1 is composed of a 5′ handle, seed region, and 3′ end (Fonfara et al., 2016; Zetsche et al., 2015), we synthesized oligonucleotides complementary to different regions of the crRNA (Figures 1 and S1). We then generated their corresponding crDuplex (Figure S1) by annealing an equimolar oligonucleotide with the crRNA.

As shown in Figure 1B, the first type of crDuplex, DNA-crRNA, was constructed by hybridization of unmodified or PS-modified DNA oligonucleotide (Figure 1A) with crRNA at different regions (crDuplex1 to crDuplex13). In the presence of plasmid encoding AsCpf1, crDuplex1 to crDuplex10 (unmodified DNA-crDuplex) retain 60% or more genome-editing activity of wild-type crRNA at the *DNMT1* locus in 293T cells (Figure 1C). However, we observed no obvious correlation between genome-editing efficiency and the hybrid region or between genome-editing efficiency and the length of oligonucleotide tested (Figure 1C). Interestingly, PS-modified DNA-crDuplex, including crDuplex11, crDuplex12, and crDuplex13, dramatically reduced genome-editing efficiency under the same condition (Figure 1C). Moreover, crDuplex11 and crDuplex13 completely blocked the function of Cpf1 (Figure 1C).

DNA and RNA oligonucleotides possess important chemical difference at the 2′ position on the ribose (Figure 1A). We then examined the second type of crDuplex, RNA-crRNA, in order to explore the effects of RNA oligonucleotides on Cpf1-mediated genome editing. In this case, unmodified, 2′-fluoro, 2′-*O*-methyl, and PS-modified RNA oligonucleotides (Figure 1A) were used to produce unmodified RNA-crRNA (crDuplex14–16), 2′-fluoro RNA-crRNA (crDuplex17 and crDuplex18), 2′-*O*-methyl RNA-crRNA (crDuplex19 and crDuplex20), and PS-modified RNA-crRNA (crDuplex21) (Figure 1D). As shown in Figure 1E, crDuplex14–16, crDuplex19, and crDuplex20 showed comparable or slightly higher genome-editing efficiency in comparison with crRNA, while crDuplex17, crDuplex18, and crDuplex21 reduced cleavage activity to a different extent, depending on the pattern of modification (Figure 1E). We noticed that 2′-fluoro RNA-crRNA (crDuplex17 and crDuplex18) suppressed genome-editing activity more potently than unmodified RNA-crRNA (crDuplex14–16) and 2′-*O*-methyl RNA-crRNA (crDuplex19 and crDuplex20). PS-modified RNA-crRNA (crDuplex21) also displayed inhibition activity, which is comparable with 2′-fluoro RNA-crRNA (crDuplex17 and crDuplex18), but not as potent as the corresponding duplex containing the PS-modified DNA oligonucleotide, crDuplex11.

Taken together, these findings suggested that genome-editing activity of the CRISPR-Cpf1 system can be affected by oligonucleotides with different chemical modifications, length of DNA or RNA oligonucleotides, and position of hybridization with crRNA. Among all the oligonucleotides tested, both 2′-fluoro RNA and PS-modified DNA exhibited apparent inhibitory effects. Given the challenge to synthesize relatively long 2′-fluoro-modified oligonucleotides, we selected two PS-modified DNA-crRNA (crDuplex11 and crDuplex13), which exhibited the most potent inhibition against Cpf1 expression plasmid (Figure 1E) for further studies. Our previous studies reported that co-delivery of chemically modified Cpf1 mRNA and crRNA improved genome-editing efficiency of Cpf1 (Li et al., 2017, 2018a). To further validate the observed inhibitory effects of crDuplex11 and crDuplex13, we delivered crDuplex in the presence of Ψ-modified Cpf1 mRNA in 293T cells. In this case, crDuplex13 exhibited detectable genome-editing activity, whereas crDuplex11 was capable of completely disabling Cpf1 function under the same condition (Figure 1F). Comparing the structures of crDuplex11 to crDuplex13, we theorized that PS-DNA oligonucleotide with the same length of crRNA may be essential to fully inhibit genome editing of Cpf1.

Switch-Off Function of PS-Modified DNA Oligonucleotides

In the study above, crDuplex11 formed between crRNA and cDNA oligonucleotide with 42 PS linkages (termed ps42DNA-DNMT1 inhibitor; Figure 2A; Table S1) was able to completely switch off the activity of Cpf1 in the hybridization form.

Figure 1. Genome-Editing Efficiency of crRNA Duplexes in Human Cells

(A) Structures of unmodified and chemically modified nucleotides used in this study.

(B) Schematic illustration of crRNA and DNA-crRNA duplexes. crRNA consists of a handle (pseudoknot structure) and a guide segment. DNA-crRNA duplexes were generated by hybridization of different lengths of unmodified (black) or phosphorothioate (PS)-modified (red) DNA oligonucleotides with various regions of the crRNA.

(C) Relative genome-editing efficiency of DNA-crRNA duplexes at the *DNMT1* gene locus in the presence of AsCpf1 plasmid in 293T cells.

(D) Schematic illustration of RNA-crRNA duplexes. RNA-crRNA duplexes were generated by hybridization of unmodified (green), 2′-fluoro (violet), or 2′-*O*-methyl (blue) modified RNA oligonucleotides with the crRNA.

(E) Relative genome-editing efficiency of RNA-crRNA duplexes at the *DNMT1* gene locus in the presence of AsCpf1 plasmid in 293T cells.

(F) Relative genome-editing efficiency of PS-DNA-crRNA duplexes at the *DNMT1* gene locus in the presence of AsCpf1 mRNA in 293T cells.

Relative genome-editing efficiency (%) in (C), (E), and (F) was determined using the T7E1 cleavage assay 48 hr post-treatment and normalized to that of the wild-type crRNA group. Data are expressed as mean ± SD from three biological replicates. *$p < 0.05$, **$p < 0.01$, and ***$p < 0.001$, two-tailed t test. ND, not detectable; NS, not significant.

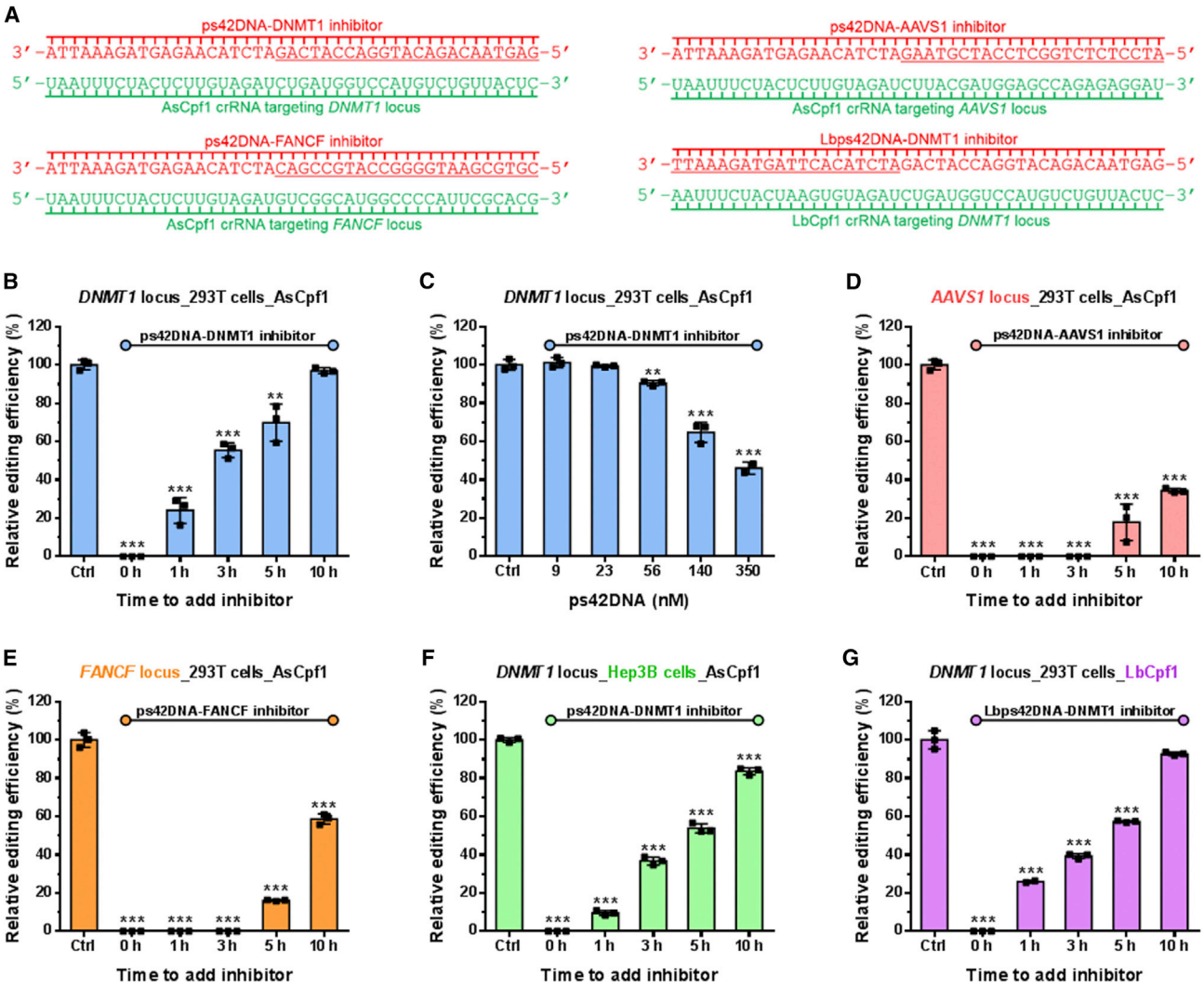

Figure 2. Inhibitory Effects of PS DNA Oligonucleotides on Cpf1-Mediated Genome Editing in Human Cells

(A) Sequences of ps42DNA inhibitors used for (B)–(G). Nucleotides in green denote crRNAs, and those in red denote corresponding ps42DNA inhibitors.

(B) Time-dependent inhibitory effects of ps42DNA-DNMT1 on AsCpf1-mediated genome editing at the *DNMT1* locus in 293T cells. "Time to add inhibitor": ps42DNA-DNMT1 was added at various time points after treatment with AsCpf1 mRNA and crRNA targeting *DNMT1* locus.

(C) Dose-dependent inhibitory effects of ps42DNA-DNMT1 on AsCpf1-mediated genome editing at the *DNMT1* locus in 293T cells. ps42DNA-DNMT1 was added 5 hr after treatment with CRISPR-Cpf1 mRNA and crRNA targeting *DNMT1* locus.

(D) Time-dependent inhibitory effects of ps42DNA-AAVS1 on AsCpf1-mediated genome editing at the *AAVS1* locus in 293T cells. "Time to add inhibitor": ps42DNA-AAVS1 was added at various time points after treatment with AsCpf1 mRNA and crRNA targeting *AAVS1* locus.

(E) Time-dependent inhibitory effects of ps42DNA-FANCF on AsCpf1-mediated genome editing at the *FANCF* locus in 293T cells. "Time to add inhibitor": ps42DNA-FANCF was added at various time points after treatment with AsCpf1 mRNA and crRNA targeting *FANCF* locus.

(F) Time-dependent inhibitory effects of ps42DNA-DNMT1 on AsCpf1-mediated genome editing at the *DNMT1* locus in Hep3B cells. "Time to add inhibitor": ps42DNA-DNMT1 was added at various time points after treatment with AsCpf1 mRNA and crRNA targeting *DNMT1* locus.

(G) Time-dependent inhibitory effects of Lbps42DNA-DNMT1 on LbCpf1-mediated genome editing at the *DNMT1* locus in 293T cells. "Time to add inhibitor": Lbps42DNA-DNMT1 was added at various time points after treatment with LbCpf1 mRNA and LbCpf1 crRNA targeting *DNMT1* locus.

The control group (Ctrl) was treated only with AsCpf1 mRNA and crRNA. The concentration of inhibitors in (B) and (D)–(G) is 140 nM (2.5-fold molar excess relative to crRNA). Relative genome-editing efficiency in (B)–(G) was determined using the T7E1 cleavage assay from three biological replicates 48 hr post-treatment, normalized to that of the control group without adding inhibitors, and plotted versus time or dose. $^{**}p < 0.01$ and $^{***}p < 0.001$ versus the control group, two-tailed t test. See Figure S2 for the corresponding gel images.

Subsequently, we speculated that such DNA oligonucleotide itself may enable us to inactivate Cpf1 activity and serve as a Cpf1 inhibitor. To test this hypothesis, we separately formulated three components (crRNA targeting *DNMT1* locus, AsCpf1 mRNA, and ps42DNA-DNMT1) using Lipofectamine 3000 reagent and then simultaneously delivered these three components to 293T

cells. Notably, the process of genome editing was effectively interrupted when ps42DNA-DNMT1 was added together with the other two components (time = 0 hr; Figure 2B). Next, we treated cells with crRNA plus AsCpf1 mRNA, followed by the addition of the inhibitor at various time points. As shown in Figure 2B, ps42DNA-DNMT1 displayed time-dependent inhibition on Cpf1-mediated genome-editing activity. At the 10 hr time point, ps42DNA-DNMT1 was not able to affect the Cpf1 function. We then investigated dose-dependent inhibitory effects of ps42DNA-DNMT1 5 hr post-treatment of CRISPR-Cpf1 components. ps42DNA-DNMT1 was found to act in a dose-dependent manner to regulate genomic cleavage (Figure 2C). These observations indicated that time and dose are two crucial factors for ps42DNA-DNMT1 to exert switch-off function for the CRISPR-Cpf1 system.

Applicability of PS DNA Oligonucleotides in Additional Gene Loci, Cell Types, and Cpf1 Orthologs

To assess the applicability of this approach, we synthesized two additional 43 nt DNA oligonucleotides (each contains 42 PS linkages) complementary to crRNAs targeting the *AAVS1* and *FANCF* genes (Kim et al., 2016a; Kleinstiver et al., 2016) (termed ps42DNA-AAVS1 and ps42DNA-FANCF, respectively; Figure 2A; Table S1). Consistent with the results mentioned above, both ps42DNA-AAVS1 and ps42DNA-FANCF showed time-dependent inhibition of genome editing for their corresponding target DNA sequences. Their inhibition potency was higher than that of ps42DNA-*DNMT1*, as evidenced by undetectable cleavage at time points 1 and 3 hr (Figures 2D and 2E).

In addition to 293T cell line, we also evaluated the effects of ps42DNA-DNMT1 in Hep3B cells (a human hepatoma cell line). Similarly, ps42DNA-DNMT1 showed dramatic inhibition of genome editing in Hep3B cells (Figure 2F). Next, we examined the same strategy for another Cpf1 ortholog, LbCpf1 (Zetsche et al., 2015), using its corresponding PS-modified DNA oligonucleotide (termed Lbps42DNA-DNMT1; Figure 2A; Table S1), which exhibited strong inhibition of genome editing in a time-dependent manner similar to ps42DNA-DNMT1 (Figure 2G). Collectively, ps42DNA oligonucleotides are broadly applicable to inhibit Cpf1-mediated genomic cleavage at different gene loci in mammalian cells.

Inhibitory Effects of PS-Modified DNA Oligonucleotides with Random Sequences on CRISPR-Cas in Human Cells

In order to explore the sequence specificity of PS-emodified DNA oligonucleotides on inhibition of Cpf1 activity, we initially examined the cross-inhibitory effects among these PS-modified DNA oligonucleotides (ps42DNA-AAVS1 and ps42DNA-FANCF, used for blocking gene editing at *AAVS1* and *FANCF* loci, respectively, were applied to the *DNMT1* locus). Both ps42DNA-AAVS1 and ps42DNA-FANCF displayed robust inhibition of Cpf1-mediated genome editing at the *DNMT1* locus (Figure 3A). Next, we designed PS-modified DNA oligonucleotides with random sequences (RAMpsDNA) and conducted the same assays in human cells. Interestingly, RAMpsDNA also completely inhibited Cpf1-mediated genome editing at three different loci tested, including *DNMT1*, *AAVS1*, and *FANCF* (Figure 3B). Moreover, such effect was observed in different cell lines ((Figure 3C) and was time dependent (Figure 3D). To rule out the possibility that such inhibitory effects were resulted from the interactions between exogenous oligonucleotides and endogenous components in cells, the unmodified DNA oligonucleotide (uDNA) previously used for crDuplex2 formation was added to cells under the same conditions. We found that uDNA did not affect Cpf1 activity (Figure S3B). Collectively, PS-modified DNA oligonucleotides are capable of blocking activity of CRISPR-Cpf1 without specific sequence requirements.

To investigate the effects of oligonucleotide length on Cpf1 activity, we subsequently examined the inhibitory effects of PS-modified DNA oligonucleotides with different lengths (30 and 100 nt, termed ps29DNA and ps99DNA on the basis of their numbers of PS linkages; Table S1) in human cells in addition to 43 nt RAMpsDNA. As shown in Figure S3H, both ps29DNA and ps99DNA displayed dramatic inhibition of Cpf1-mediated genome editing activities in cells but weaker than RAMpsDNA. Because ribonucleoprotein complex (RNP) is an alternative method for genome editing, we also evaluated RAMpsDNA inhibition on Cpf1 RNP. Notably, the activity of preassembled Cpf1 RNP was fully inhibited within 5 hr (Figure S3I).

Last, to test the inhibition applicability of PS DNA to the CRISPR-Cas9 system, we synthesized a 100 nt PS DNA oligonucleotides (ps99DNA) complementary to the full-length synthetic SpCas9 single-guide RNA (sgRNA) targeting the *EMX1* gene (Table S1). As shown in Figure S4A, the genome-editing activity of SpCas9 was dramatically lowered but not totally inhibited when ps99DNA was added to 293T cells. Nevertheless, ps99DNA almost completely inactivated SpCas9 activity in Hep3B cells (Figure S4B). Next, we evaluated the ps99DNA activity at two additional gene loci, *RELA* and *CDC42BPB*. Under this condition, the ps99DNA is considered as a randomized DNA oligonucleotide for these two loci. Similar effects were observed for the inhibition of SpCas9 in both 293T and Hep3B cells regardless of sgRNA used (Figure S4; Table S1).

Interaction of Cpf1 with Oligonucleotides

Previous reports showed that Cpf1 protein and crRNA first formed a binary complex and then exerted a conformational change to the Cpf1-crRNA-target DNA ternary complex (Gao et al., 2016). To study the interaction between Cpf1 protein and the PS-modified DNA oligonucleotide, we performed an electrophoretic mobility shift assay (EMSA) using AsCpf1 protein. As shown in Figure 4A, after incubation of crRNA with increased concentrations of Cpf1 protein, a new band appeared at a higher position, indicating the complex formation between Cpf1 protein and crRNA. A similar band was found in the experiment using ps42DNA, which suggested that ps42DNA interacted with Cpf1 protein with a comparable affinity to crRNA (Figure 4B). In contrast, uDNA was cleaved after exposure to high concentrations of Cpf1 protein (Figure S5A). These results were analogous to a recent report that FnCpf1 protein non-specifically degrades single-stranded DNA in the absence of crRNA (Sundaresan et al., 2017) and explained the activity differences between PS-modified DNA and

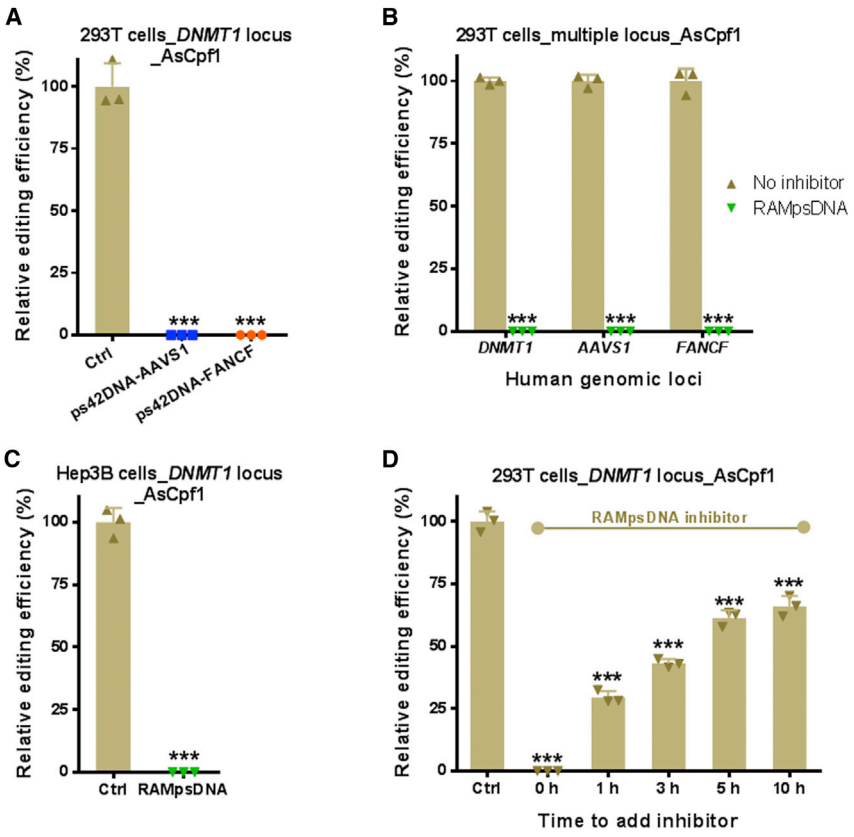

Figure 3. Inhibitory Effects of PS-Modified DNA Oligonucleotides with Random Sequences on Cpf1-Mediated Genome Editing in Human Cells

(A) Inhibitory effects of ps42DNA-AAVS1 and ps42DNA-FANCF on AsCpf1-mediated genome editing at the *DNMT1* locus in 293T cells. ps42DNA-AAVS1 or ps42DNA-FANCF was added simultaneously with AsCpf1 mRNA and AsCpf1 crRNA targeting *DNMT1* locus.

(B) Inhibitory effects of RAMpsDNA on AsCpf1-mediated genome editing at the *DNMT1*, *AAVS1*, and *FANCF* loci in 293T cells. RAMpsDNA was added simultaneously with CRISPR-Cpf1 mRNA and crRNA.

(C) Inhibitory activity of RAMpsDNA on AsCpf1-mediated genome editing at the *DNMT1* locus in Hep3B cells. RAMpsDNA was added simultaneously with CRISPR-Cpf1 mRNA and crRNA targeting *DNMT1* locus.

(D) Time-dependent inhibitory effects of RAMpsDNA on AsCpf1-mediated genome editing at the *DNMT1* locus in 293T cells. "Time to add inhibitor": RAMpsDNA was added at various time points after treatment with AsCpf1 mRNA and crRNA targeting *DNMT1* locus.

The control group (Ctrl) was treated only with AsCpf1 mRNA and crRNA. The concentration of inhibitors is 140 nM (2.5-fold molar excess relative to crRNA). Relative genome-editing efficiency in (A)–(D) was determined using the T7E1 cleavage assay from three biological replicates 48 hr post-treatment and normalized to that of the control group without adding inhibitors. ***$p < 0.001$ versus the control group, two-tailed t test. See Figure S3 for the corresponding gel images.

unmodified DNA. Additionally, gel electrophoresis analysis of the mixture of Cpf1 protein, crRNA, and ps42DNA indicated that these three components were assembled into Cpf1-crRNA-ps42DNA ternary complex (Figure 4C). A similar trend was observed when crDuplex11 (hybridized from crRNA and ps42DNA) was used (Figure S5B).

Inhibitory Effects of PS-Modified DNA Oligonucleotides on Cpf1/crRNA Ribonucleoprotein *In Vitro*

Cpf1 uses a single-stranded crRNA to recognize and cleave target DNA (Dong et al., 2016; Fonfara et al., 2016; Gao et al., 2016; Stella et al., 2017; Swarts et al., 2017; Yamano et al., 2016; Zetsche et al., 2015). In order to mimic genome editing in cell studies, the *DNMT1* genomic region was amplified by PCR and used as a double-stranded DNA substrate. We first mixed Cpf1, crRNA, and DNA substrate to examine the *in vitro* reaction condition. As we increased the amount of Cpf1 protein, more cleaved fragments were observed (Figure S5C). To further investigate the inhibitory effects, we added ps42DNA into the reaction mixture at different time points using a fixed molar ratio of 1:8:1 (crRNA/Cpf1 protein/DNA substrate). We found that ps42DNA inactivated Cpf1 protein in a time-dependent manner (Figure S5D, left), which was consistent with our observation in the cell studies. The same effect was observed when Cpf1 protein and crRNA pre-assembled into RNP (Figure S5D, right). Because this *in vitro* reaction does not require extra time for Cpf1 protein production, the time frame ranges in minutes.

PS-Modified DNA Oligonucleotides Blocked Target DNA Binding and Recognition by the Cpf1 Nuclease

In order to distinguish different components in the Cpf1 system, we first labeled the 3′ end of crRNA with a Cy5 fluorescent probe (termed Cy5crRNA) and examined its function in 293T cells. Cy5crRNA showed equivalent activity to crRNA, indicating that Cy5 probe has little influence on crRNA activity and is suitable for the mechanism study (Figure S5E). We subsequently carried out *in vitro* cleavage assay using Cy5crRNA to visualize the interactions between cleaved DNA fragments and crRNA-Cpf1 complex. As displayed in Figure 5A under a SYBR green filter, the short cleaved fragment (lane 4, white arrow) in the reaction mixture terminated by Proteinase K shifted to a higher position (lane 6, white arrow) compared to that without treatment of Proteinase K. Meanwhile, we noticed that this shifted band displayed Cy5 fluorescent signal under a Cy5 filter, suggesting the existence of crRNA (Figure 5A, lane 6, middle). In Figure 5B, we conducted the reactions with crRNA, crRNA-uDNA duplex, or crRNA-ps42DNA duplex in the absence of Proteinase K and then imaged the gel via both SYBR green and Coomassie blue staining (Figure 5B). The images in Figures 5A and 5B reflect

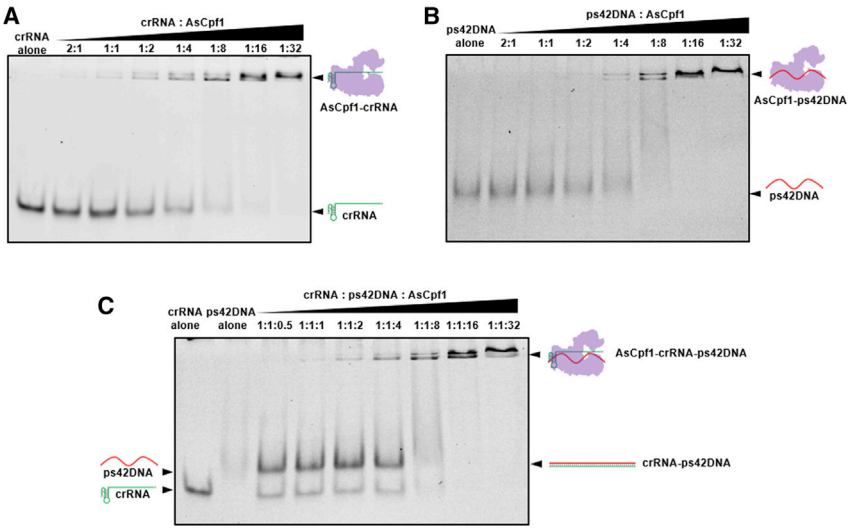

Figure 4. Interactions between Cpf1 and Oligonucleotides

(A) Complex formation between AsCpf1 protein and crRNA.

(B) Complex formation between AsCpf1 protein and ps42DNA.

(C) Complex formation of AsCpf1 protein, crRNA, and ps42DNA.

the complex formation of the crRNA, Cpf1 protein, and the short cleaved DNA fragment.

As illustrated in Figure 5C, in the presence of Proteinase K, three components are released from the complex, including crRNA and two cleaved DNA fragments. On the contrary, with no treatment with Proteinase K, the short cleaved DNA fragment with intensive interactions with crRNA and Cpf1 is still bounded in the ternary complex. Therefore, this DNA band (short cleaved fragment) shifted from the position less than 400 bp as shown in the ladder to the position more than 500 bp, while the other DNA fragment (long cleaved fragment) remained at the same position in the gel (Figures 5A and 5B). We subsequently quantified the amount of the uncleaved DNA substrate in Figure 5B by band intensity under a SYBR green filter in comparison with the same amount of untreated DNA substrate. We found that DNA substrate remaining in both crRNA and crRNA-uDNA groups was much lower than that in the untreated group, while the amount of DNA substrate in the group of crRNA-ps42DNA displayed no significant reduction compared with the DNA substrate alone group (Figure 5B, top). In addition, no additional band of Cpf1 protein-DNA substrate complex was detected from the gel stained by Coomassie blue (Figure 5B, bottom). Next, we studied the effects of ps42DNA (without prehybridization) and RAMpsDNA on Cpf1 and DNA substrate binding. We incubated crRNA, Cpf1, DNA substrate, and ps42DNA (or RAMpsDNA) at 37°C for 30 min. Consistent results were obtained as mentioned above (Figure S5F). These results indicated that PS-modified DNA oligonucleotides, regardless of their sequences, blocked the binding of Cpf1 protein with the DNA substrate.

Taken together, we propose the following mechanism of action (Figure 5D). Typically, Cpf1 forms regular complex with crRNA. Addition of uDNA to the complex has little effect on the recognition of target DNA substrate. uDNA may be degraded via Cpf1-mediated non-specific cleavage. In contrast to uDNA, PS-modified DNA oligonucleotides may lead to a new complex with Cpf1 and crRNA, consequently blocking the binding to target DNA substrate, thereby inactivating the function of Cpf1.

DISCUSSION

Bacteria and phages are the natural sources of Acr proteins (Borges et al., 2017; Dong et al., 2017; Harrington et al., 2017; Hynes et al., 2017, 2018; Landsberger et al., 2018; Marino et al., 2018; Maxwell, 2017; Pawluk et al., 2016a, 2016b; Rauch et al., 2017; Shin et al., 2017; Watters et al., 2018; Yang and Patel, 2017). Recently, more and more naturally occurring Acr proteins were reported to be effective CRISPR inhibitors in human cells (Borges et al., 2017; Dong et al., 2017; Harrington et al., 2017; Hynes et al., 2017, 2018; Landsberger et al., 2018; Marino et al., 2018; Maxwell, 2017; Pawluk et al., 2016a, 2016b; Rauch et al., 2017; Shin et al., 2017; Watters et al., 2018; Yang and Patel, 2017). In this study, we synthesized a series of oligonucleotides and found that PS-modified DNA oligonucleotides with equal length to crRNA, while independent of their sequences, were able to inhibit Cpf1 activity. On the basis of the present results, we summarized a list of structure-activity relationships for modulating Cpf1 function: (1) In general, unmodified DNA and RNA oligonucleotides showed moderate effects on Cpf1-mediated genome-editing activity regardless of the hybrid region and the length of oligonucleotides tested. (2) 2′-Fluoro-modified oligonucleotides substantially interfered with Cpf1-mediated cleavage. (3) 2′-*O*-methyl-modified oligonucleotides maintained the performance of the wild-type crRNA. (4) PS-modified DNA oligonucleotides can act as potent inhibitors to switch off Cpf1 function. Most important, these PS-modified DNA oligonucleotides enabled us to inhibit genome editing activities of AsCpf1, LbCpf1, and SpCas9. Also, the inhibition was observed in three human genomic loci in a time- and dose-dependent manner. Further investigation of the sequence of PS-modified DNA oligonucleotides revealed that the inhibitory effects on Cpf1 activity were sequence-independent for inhibiting Cpf1 activity with an optimal length of 43 nt in this study.

Previous studies reported that a conformational change occurs from the Cpf1-crRNA binary state to the Cpf1-crRNA-DNA ternary complex (Gao et al., 2016). This structural transition facilitates the seed segment of crRNA developing an A-form conformation in order to pair with target DNA and thereby inducing gene cutting (Gao et al., 2016). In this study, EMSAs showed that Cpf1 protein was able to bind to the single-stranded PS-modified DNA oligonucleotide. The inhibition activity was noticed within 20 min after Cpf1 protein was present. Hence, the time window to stop Cpf1 functions is within the range of

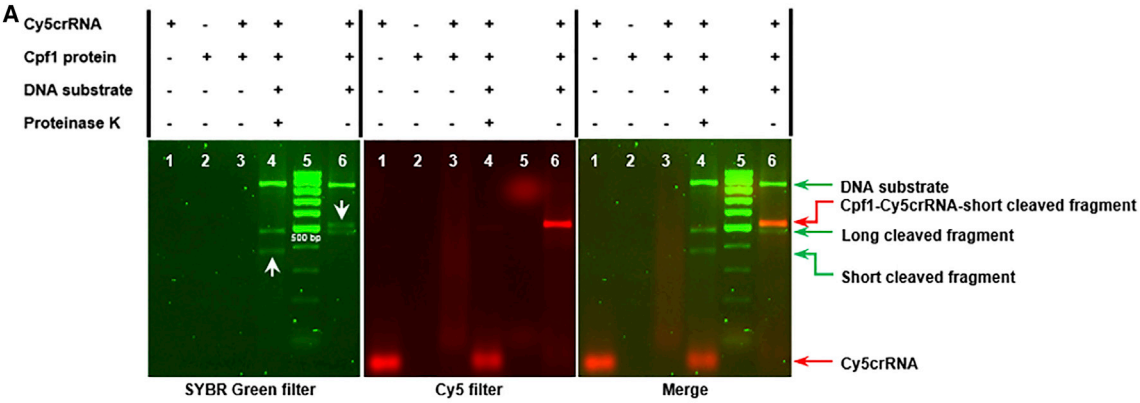

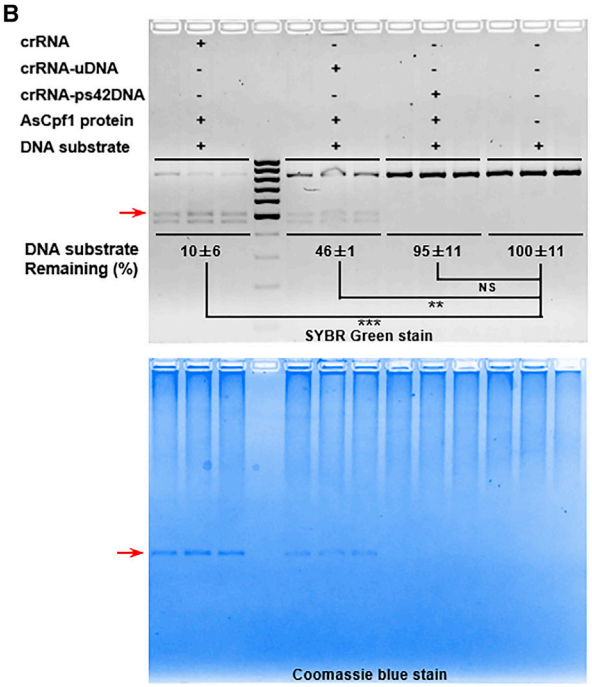

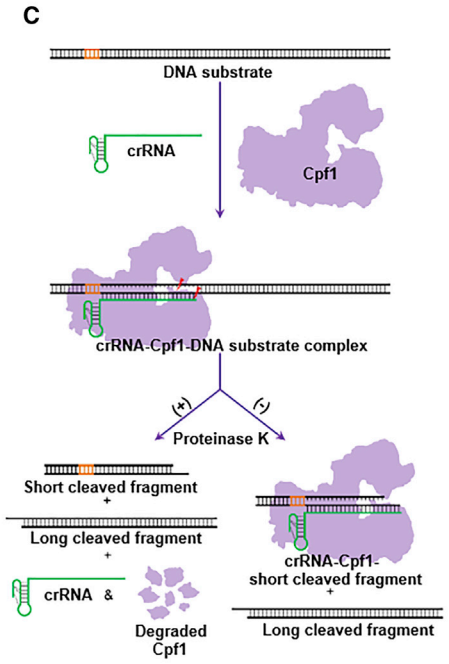

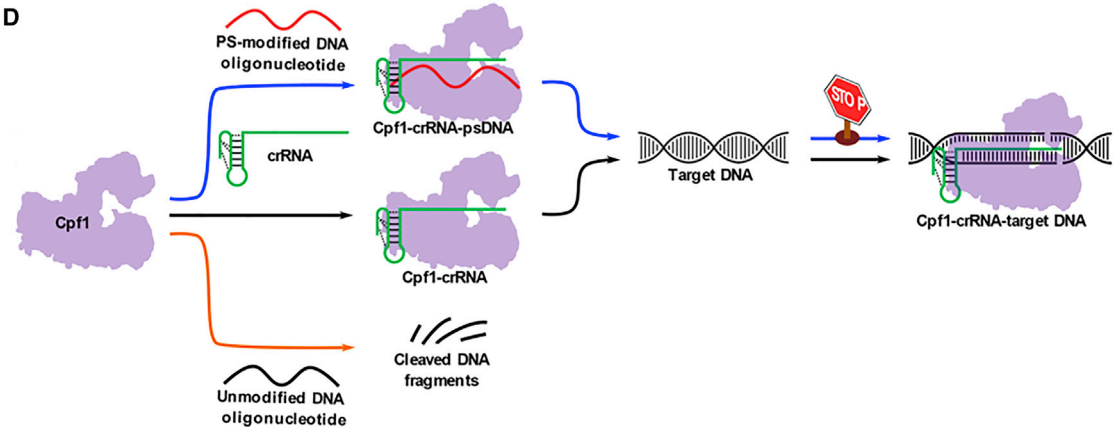

(legend on next page)

minutes. Yet these PS-modified DNA oligonucleotides can prevent the gene editing of Cpf1 plasmid and mRNA during the translation process. Through co-localization and quantification analysis, we speculate that PS-modified DNA oligonucleotides may hinder target DNA binding and recognition by the Cpf1 nuclease. Overall, the findings of anti-Cpf1 oligonucleotides expand the source of Cpf1 inhibitors. These synthetic oligonucleotides, together with naturally occurring Acr proteins, provide useful tools to further understand and modulate the CRISPR-Cpf1 system. Both types of inhibitors are able to inhibit Cpf1 functions in human cells in a target sequence-independent manner. In case acute toxic effects of the CRISPR system occur in clinical use, the combination of anti-Cpf1 proteins and oligonucleotides may serve as antidotes.

STAR★METHODS

Detailed methods are provided in the online version of this paper and include the following:

- KEY RESOURCES TABLE
- CONTACT FOR REAGENT AND RESOURCE SHARING
- EXPERIMENTAL MODEL AND SUBJECT DETAILS
  - Cell Lines and Cell Culture
- METHOD DETAILS
  - Preparation of crDuplex
  - Co-delivery of CRISPR components into human cells
  - Time- and dose-dependent inhibitory effects of PS-modified DNA oligonucleotides
  - T7E1 enzymatic cleavage assays
  - EMSAs
  - Cpf1-mediated *in vitro* cleavage assays
  - Inhibition of Cpf1 cleavage activity *in vitro*
  - Visualization of Cpf1 protein, crRNA, and DNA substrate
- QUANTIFICATION AND STATISTICAL ANALYSIS

SUPPLEMENTAL INFORMATION

Supplemental Information includes five figures and two tables and can be found with this article online at https://doi.org/10.1016/j.celrep.2018.11.079.

ACKNOWLEDGMENTS

This work was supported by the NIH through the National Heart, Lung, and Blood Institute (grant R01HL136652), as well as by the start-up fund from the College of Pharmacy at The Ohio State University. We acknowledge F. Zhang at the Broad Institute of MIT and Harvard University for kindly providing the AsCpf1 plasmid. We thank T. Nakane, H. Nishimasu, and O. Nureki at the University of Tokyo for helpful discussion and technical assistance.

AUTHOR CONTRIBUTIONS

B.L. designed and performed all experiments, analyzed data, and wrote the manuscript. C. Zeng and W.L. designed and performed experiments related to *in vitro* cleavage assay. X.Z. designed and conducted fluorescence analysis. X.L., W.Z., and C. Zhang conducted cell analysis. Y.D. conceived and supervised the project and wrote the manuscript. The final manuscript was edited and approved by all authors.

DECLARATION OF INTERESTS

The authors declare no competing interests.

Received: May 10, 2018
Revised: September 12, 2018
Accepted: November 20, 2018
Published: December 18, 2018

REFERENCES

Bin Moon, S., Lee, J.M., Kang, J.G., Lee, N.E., Ha, D.I., Kim, D.Y., Kim, S.H., Yoo, K., Kim, D., Ko, J.H., and Kim, Y.S. (2018). Highly efficient genome editing by CRISPR-Cpf1 using CRISPR RNA with a uridinylate-rich 3′-overhang. Nat. Commun. *9*, 3651.

Borges, A.L., Davidson, A.R., and Bondy-Denomy, J. (2017). The discovery, mechanisms, and evolutionary impact of anti-CRISPRs. Annu. Rev. Virol. *4*, 37–59.

Bosley, K.S., Botchan, M., Bredenoord, A.L., Carroll, D., Charo, R.A., Charpentier, E., Cohen, R., Corn, J., Doudna, J., Feng, G., et al. (2015). CRISPR germline engineering–the community speaks. Nat. Biotechnol. *33*, 478–486.

Chow, R.D., Kim, H.R., and Chen, S. (2018). Programmable sequential mutagenesis by inducible Cpf1 crRNA array inversion. Nat. Commun. *9*, 1903.

Dang, Y., Jia, G., Choi, J., Ma, H., Anaya, E., Ye, C., Shankar, P., and Wu, H. (2015). Optimizing sgRNA structure to improve CRISPR-Cas9 knockout efficiency. Genome Biol. *16*, 280.

Figure 5. Mechanistic Studies for PS-Modified DNA Oligonucleotides on Cpf1-Mediated Genome Editing

(A) Analysis of fluorescently (Cy5) labeled crRNA-mediated *in vitro* cleavage reactions under SYBR (left) and Cy5 (middle) filters. A merged image is shown at right. The two white arrows in the left image indicate the band shift from lane 4 (apparent size < 500 bp) in the presence of Proteinase K to that in lane 6 (apparent size > 500 bp) in the absence of Proteinase K.

(B) Top: quantification of DNA substrate bound with AsCpf1 in the presence of crRNA, crRNA-uDNA, or crRNA-ps42DNA. The uncleaved DNA substrate was quantified by densitometric analysis and normalized to the untreated DNA substrate. Data represent the normalized percentage of DNA substrate remaining (**$p < 0.01$ and ***$p < 0.001$, two-tailed t test; NS, not significant). Bottom: localization of the complex of Cpf1, crRNA, and the short cleaved DNA fragment by Coomassie blue staining. The red arrow denotes the complex composed of AsCpf1 protein, crRNA, and the short cleaved fragment.

(C) Illustration of Cpf1-mediated *in vitro* cleavage reactions with and without Proteinase K digestion. After the formation of crRNA-Cpf1-target DNA ternary complex, DNA substrate is cleaved. With the addition of Proteinase K, crRNA and two cleaved DNA fragments are released from the complex. Nevertheless, in the absence of Proteinase K, one DNA fragment (long cleaved fragment) without extensive interactions with crRNA and AsCpf1 protein is released from the ternary complex. The remaining ternary complex consists of AsCpf1 protein, crRNA, and the other DNA fragment (the short cleaved fragment).

(D) Proposed mechanism of inhibition for the CRISPR-Cpf1 using PS-modified DNA oligonucleotides. Normally, Cpf1 endonuclease is guided by single crRNA to recognize target DNA and induce DNA double-strand breaks (black pathway in the middle). Regarding uDNA, it has little effects on Cpf1-mediated genome editing, which may be the consequence of non-specific degradation by Cpf1 (orange pathway at the bottom). In the case of PS-modified DNA, after it interacts with Cpf1 and crRNA, the new complex cannot recognize DNA substrate, consequently inactivating genome editing (blue pathway at the top).

Deleavey, G.F., and Damha, M.J. (2012). Designing chemically modified oligonucleotides for targeted gene silencing. Chem. Biol. *19*, 937–954.

DeLorenzo, D.M., Rottinghaus, A.G., Henson, W.R., and Moon, T.S. (2018). Molecular toolkit for gene expression control and genome modification in Rhodococcus opacus PD630. ACS Synth. Biol. *7*, 727–738.

Dong, D., Ren, K., Qiu, X., Zheng, J., Guo, M., Guan, X., Liu, H., Li, N., Zhang, B., Yang, D., et al. (2016). The crystal structure of Cpf1 in complex with CRISPR RNA. Nature *532*, 522–526.

Dong, D., Guo, M., Wang, S., Zhu, Y., Wang, S., Xiong, Z., Yang, J., Xu, Z., and Huang, Z. (2017). Structural basis of CRISPR-SpyCas9 inhibition by an anti-CRISPR protein. Nature *546*, 436–439.

Endo, A., Masafumi, M., Kaya, H., and Toki, S. (2016). Efficient targeted mutagenesis of rice and tobacco genomes using Cpf1 from Francisella novicida. Sci. Rep. *6*, 38169.

Fonfara, I., Richter, H., Bratovič, M., Le Rhun, A., and Charpentier, E. (2016). The CRISPR-associated DNA-cleaving enzyme Cpf1 also processes precursor CRISPR RNA. Nature *532*, 517–521.

Gao, P., Yang, H., Rajashankar, K.R., Huang, Z., and Patel, D.J. (2016). Type V CRISPR-Cas Cpf1 endonuclease employs a unique mechanism for crRNA-mediated target DNA recognition. Cell Res. *26*, 901–913.

Harrington, L.B., Doxzen, K.W., Ma, E., Liu, J.J., Knott, G.J., Edraki, A., Garcia, B., Amrani, N., Chen, J.S., Cofsky, J.C., et al. (2017). A broad-spectrum inhibitor of CRISPR-Cas9. Cell *170*, 1224–1233.e15.

Hendel, A., Bak, R.O., Clark, J.T., Kennedy, A.B., Ryan, D.E., Roy, S., Steinfeld, I., Lunstad, B.D., Kaiser, R.J., Wilkens, A.B., et al. (2015). Chemically modified guide RNAs enhance CRISPR-Cas genome editing in human primary cells. Nat. Biotechnol. *33*, 985–989.

Hur, J.K., Kim, K., Been, K.W., Baek, G., Ye, S., Hur, J.W., Ryu, S.M., Lee, Y.S., and Kim, J.S. (2016). Targeted mutagenesis in mice by electroporation of Cpf1 ribonucleoproteins. Nat. Biotechnol. *34*, 807–808.

Hynes, A.P., Rousseau, G.M., Lemay, M.L., Horvath, P., Romero, D.A., Fremaux, C., and Moineau, S. (2017). An anti-CRISPR from a virulent streptococcal phage inhibits Streptococcus pyogenes Cas9. Nat. Microbiol. *2*, 1374–1383.

Hynes, A.P., Rousseau, G.M., Agudelo, D., Goulet, A., Amigues, B., Loehr, J., Romero, D.A., Fremaux, C., Horvath, P., Doyon, Y., et al. (2018). Widespread anti-CRISPR proteins in virulent bacteriophages inhibit a range of Cas9 proteins. Nat. Commun. *9*, 2919.

Juliano, R.L. (2016). The delivery of therapeutic oligonucleotides. Nucleic Acids Res. *44*, 6518–6548.

Kim, D., Kim, J., Hur, J.K., Been, K.W., Yoon, S.H., and Kim, J.S. (2016a). Genome-wide analysis reveals specificities of Cpf1 endonucleases in human cells. Nat. Biotechnol. *34*, 863–868.

Kim, Y., Cheong, S.A., Lee, J.G., Lee, S.W., Lee, M.S., Baek, I.J., and Sung, Y.H. (2016b). Generation of knockout mice by Cpf1-mediated gene targeting. Nat. Biotechnol. *34*, 808–810.

Kim, H., Kim, S.T., Ryu, J., Kang, B.C., Kim, J.S., and Kim, S.G. (2017). CRISPR/Cpf1-mediated DNA-free plant genome editing. Nat. Commun. *8*, 14406.

Kleinstiver, B.P., Tsai, S.Q., Prew, M.S., Nguyen, N.T., Welch, M.M., Lopez, J.M., McCaw, Z.R., Aryee, M.J., and Joung, J.K. (2016). Genome-wide specificities of CRISPR-Cas Cpf1 nucleases in human cells. Nat. Biotechnol. *34*, 869–874.

Landsberger, M., Gandon, S., Meaden, S., Rollie, C., Chevallereau, A., Chabas, H., Buckling, A., Westra, E.R., and van Houte, S. (2018). Anti-CRISPR phages cooperate to overcome CRISPR-Cas immunity. Cell *174*, 908–916.e12.

Latorre, A., Latorre, A., and Somoza, Á. (2016). Modified RNAs in CRISPR/Cas9: An Old Trick Works Again. Angew. Chem. Int. Ed. Engl. *55*, 3548–3550.

Lee, Y.J., Hoynes-O'Connor, A., Leong, M.C., and Moon, T.S. (2016). Programmable control of bacterial gene expression with the combined CRISPR and antisense RNA system. Nucleic Acids Res. *44*, 2462–2473.

Lee, K., Mackley, V.A., Rao, A., Chong, A.T., Dewitt, M.A., Corn, J.E., and Murthy, N. (2017). Synthetically modified guide RNA and donor DNA are a versatile platform for CRISPR-Cas9 engineering. eLife *6*, e25312.

Li, B., Luo, X., and Dong, Y. (2016). Effects of chemically modified messenger RNA on protein expression. Bioconjug. Chem. *27*, 849–853.

Li, B., Zhao, W., Luo, X., Zhang, X., Li, C., Zeng, C., and Dong, Y. (2017). Engineering CRISPR-Cpf1 crRNAs and mRNAs to maximize genome editing efficiency. Nat. Biomed. Eng. *1*, 0066.

Li, B., Zeng, C., and Dong, Y. (2018a). Design and assessment of engineered CRISPR-Cpf1 and its use for genome editing. Nat. Protoc. *13*, 899–914.

Li, X., Wang, Y., Liu, Y., Yang, B., Wang, X., Wei, J., Lu, Z., Zhang, Y., Wu, J., Huang, X., et al. (2018b). Base editing with a Cpf1-cytidine deaminase fusion. Nat. Biotechnol. *36*, 324–327.

Lin, L., He, X., Zhao, T., Gu, L., Liu, Y., Liu, X., Liu, H., Yang, F., Tu, M., Tang, L., et al. (2018). Engineering the direct repeat sequence of crRNA for optimization of FnCpf1-mediated genome editing in human cells. Mol. Ther. *26*, 2650–2657.

Marino, N.D., Zhang, J.Y., Borges, A.L., Sousa, A.A., Leon, L.M., Rauch, B.J., Walton, R.T., Berry, J.D., Joung, J.K., Kleinstiver, B.P., et al. (2018). Discovery of widespread type I and type V CRISPR-Cas inhibitors. Science *362*, 240–242.

Maxwell, K.L. (2017). The anti-CRISPR story: a battle for survival. Mol. Cell *68*, 8–14.

Moreno-Mateos, M.A., Fernandez, J.P., Rouet, R., Vejnar, C.E., Lane, M.A., Mis, E., Khokha, M.K., Doudna, J.A., and Giraldez, A.J. (2017). CRISPR-Cpf1 mediates efficient homology-directed repair and temperature-controlled genome editing. Nat. Commun. *8*, 2024.

Nuñez, J.K., Harrington, L.B., and Doudna, J.A. (2016). Chemical and biophysical modulation of Cas9 for tunable genome engineering. ACS Chem. Biol. *11*, 681–688.

Park, H.M., Liu, H., Wu, J., Chong, A., Mackley, V., Fellmann, C., Rao, A., Jiang, F., Chu, H., Murthy, N., and Lee, K. (2018). Extension of the crRNA enhances Cpf1 gene editing in vitro and in vivo. Nat. Commun. *9*, 3313.

Pawluk, A., Amrani, N., Zhang, Y., Garcia, B., Hidalgo-Reyes, Y., Lee, J., Edraki, A., Shah, M., Sontheimer, E.J., Maxwell, K.L., et al. (2016a). Naturally occurring off-switches for CRISPR-Cas9. Cell *167*, 1829–1838.e9.

Pawluk, A., Staals, R.H., Taylor, C., Watson, B.N., Saha, S., Fineran, P.C., Maxwell, K.L., and Davidson, A.R. (2016b). Inactivation of CRISPR-Cas systems by anti-CRISPR proteins in diverse bacterial species. Nat. Microbiol. *1*, 16085.

Rauch, B.J., Silvis, M.R., Hultquist, J.F., Waters, C.S., McGregor, M.J., Krogan, N.J., and Bondy-Denomy, J. (2017). Inhibition of CRISPR-Cas9 with bacteriophage proteins. Cell *168*, 150–158.e10.

Richter, F., Fonfara, I., Gelfert, R., Nack, J., Charpentier, E., and Möglich, A. (2017). Switchable Cas9. Curr. Opin. Biotechnol. *48*, 119–126.

Shin, J., Jiang, F., Liu, J.J., Bray, N.L., Rauch, B.J., Baik, S.H., Nogales, E., Bondy-Denomy, J., Corn, J.E., and Doudna, J.A. (2017). Disabling Cas9 by an anti-CRISPR DNA mimic. Sci. Adv. *3*, e1701620.

Stella, S., Alcón, P., and Montoya, G. (2017). Structure of the Cpf1 endonuclease R-loop complex after target DNA cleavage. Nature *546*, 559–563.

Sundaresan, R., Parameshwaran, H.P., Yogesha, S.D., Keilbarth, M.W., and Rajan, R. (2017). RNA-independent DNA cleavage activities of Cas9 and Cas12a. Cell Rep. *21*, 3728–3739.

Swarts, D.C., van der Oost, J., and Jinek, M. (2017). Structural basis for guide RNA processing and seed-dependent DNA targeting by CRISPR-Cas12a. Mol. Cell *66*, 221–233.e4.

Tang, X., Lowder, L.G., Zhang, T., Malzahn, A.A., Zheng, X., Voytas, D.F., Zhong, Z., Chen, Y., Ren, Q., Li, Q., et al. (2017). A CRISPR-Cpf1 system for efficient genome editing and transcriptional repression in plants. Nat. Plants *3*, 17018.

Wan, W.B., and Seth, P.P. (2016). The medicinal chemistry of therapeutic oligonucleotides. J. Med. Chem. *59*, 9645–9667.

Wang, M., Mao, Y., Lu, Y., Tao, X., and Zhu, J.K. (2017). Multiplex gene editing in rice using the CRISPR-Cpf1 system. Mol. Plant *10*, 1011–1013.

Watters, K.E., Fellmann, C., Bai, H.B., Ren, S.M., and Doudna, J.A. (2018). Systematic discovery of natural CRISPR-Cas12a inhibitors. Science *362*, 236–239.

Watts, J.K., Deleavey, G.F., and Damha, M.J. (2008). Chemically modified siRNA: tools and applications. Drug Discov. Today *13*, 842–855.

Xu, R., Qin, R., Li, H., Li, D., Li, L., Wei, P., and Yang, J. (2017). Generation of targeted mutant rice using a CRISPR-Cpf1 system. Plant Biotechnol. J. *15*, 713–717.

Yamano, T., Nishimasu, H., Zetsche, B., Hirano, H., Slaymaker, I.M., Li, Y., Fedorova, I., Nakane, T., Makarova, K.S., Koonin, E.V., et al. (2016). Crystal structure of Cpf1 in complex with guide RNA and target DNA. Cell *165*, 949–962.

Yang, H., and Patel, D.J. (2017). Inhibition mechanism of an anti-CRISPR suppressor AcrIIA4 targeting SpyCas9. Mol. Cell *67*, 117–127.e5.

Ye, L., Wang, C., Hong, L., Sun, N., Chen, D., Chen, S., and Han, F. (2018). Programmable DNA repair with CRISPRa/i enhanced homology-directed repair efficiency with a single Cas9. Cell Discov. *4*, 46.

Zetsche, B., Gootenberg, J.S., Abudayyeh, O.O., Slaymaker, I.M., Makarova, K.S., Essletzbichler, P., Volz, S.E., Joung, J., van der Oost, J., Regev, A., et al. (2015). Cpf1 is a single RNA-guided endonuclease of a class 2 CRISPR-Cas system. Cell *163*, 759–771.

Zetsche, B., Heidenreich, M., Mohanraju, P., Fedorova, I., Kneppers, J., DeGennaro, E.M., Winblad, N., Choudhury, S.R., Abudayyeh, O.O., Gootenberg, J.S., et al. (2017). Multiplex gene editing by CRISPR-Cpf1 using a single crRNA array. Nat. Biotechnol. *35*, 31–34.

Zhang, Y., Long, C., Li, H., McAnally, J.R., Baskin, K.K., Shelton, J.M., Bassel-Duby, R., and Olson, E.N. (2017). CRISPR-Cpf1 correction of muscular dystrophy mutations in human cardiomyocytes and mice. Sci. Adv. *3*, e1602814.

STAR★METHODS

KEY RESOURCES TABLE

REAGENT or RESOURCE	SOURCE	IDENTIFIER
Chemicals, Peptides, and Recombinant Proteins		
Lipofectamine 3000 Transfection Reagent	Thermo Fisher Scientific	Cat#L3000015
Opti-MEM, Reduced Serum Medium	Thermo Fisher Scientific	Cat#31985070
Q5 Hot Start High-Fidelity Master Mix	New England Biolabs	Cat#M0494L
T7 Endonuclease I	New England Biolabs	Cat#M0302L
AsCpf1 protein	New England Biolabs	Gift
SYBR Safe DNA Gel Stain	Thermo Fisher Scientific	Cat#S33102
NEBuffer 3.1	New England Biolabs	Cat#B7203S
Proteinase K (component of DNeasy Blood & Tissue Kit)	QIAGEN	Cat#69506
AsCpf1 mRNAs	TriLink BioTechnologies	Custom order
LbCpf1 mRNAs	TriLink BioTechnologies	Custom order
SpCas9 mRNAs	TriLink BioTechnologies	Custom order
Experimental Models: Cell Lines		
Human: 293T cells	ATCC	CRL-3216
Human: Hep3B cells	ATCC	HB-8064
Oligonucleotides		
AsCpf1 crRNAs	TriLink BioTechnologies	Custom order
LbCpf1 crRNAs	TriLink BioTechnologies	Custom order
SpCas9 sgRNAs	Synthego	Custom order
Unmodified ssDNA oligonucleotides (see Table S1 for sequences)	Eurofins Genomics	Custom order
Chemically modified ssDNA oligonucleotides (see Table S1 for sequences)	Integrated DNA Technologies	Custom order
Unmodified ssRNA oligonucleotides (see Table S1 for sequences)	TriLink BioTechnologies	Custom order
Chemically modified ssRNA oligonucleotides (see Table S1 for sequences)	Integrated DNA Technologies	Custom order
Cy5-labeled crRNA	Integrated DNA Technologies	Custom order
Primers (see Table S2 for sequences)	Eurofins Genomics	Custom order
Recombinant DNA		
Plasmid: pcDNA3.1-hAsCpf1	Feng Zhang, the Broad Institute of MIT and Harvard	N/A
Software and Algorithms		
Imaging Lab	Bio-Rad	Version 5.2.1
Prism	GraphPad Software	GraphPad Prism 6

CONTACT FOR REAGENT AND RESOURCE SHARING

Further information and requests for resources and reagents should be directed to and will be fulfilled by the Lead Contact, Yizhou Dong (dong.525@osu.edu).

EXPERIMENTAL MODEL AND SUBJECT DETAILS

Cell Lines and Cell Culture

293T cells (ATCC) were cultured in Dulbecco's Modified Eagle's Medium (Corning Incorporated) supplemented with 10% FBS. Hep3B cells (ATCC) were cultured in Eagle's Minimum Essential Medium with 10% FBS. All cell lines were maintained at 37°C in a 5% CO2 incubator.

METHOD DETAILS

Preparation of crDuplex

crRNAs and sgRNA in Table S1 were synthesized via a solid-phase DNA/RNA synthesizer, purified by polyacrylamide gel electrophoresis system, and characterized by electrospray-ionization mass spectrometry. crDuplex (crDuplex1-21, Figure S1) were generated by hybridization of an equivalent molar AsCpf1 crRNA targeting *DNMT1* and the customized oligonucleotides (Table S1). The mixture was heated to 95°C for 30 s in Tris-EDTA buffer, followed by gradient cooling to room temperate at a rate of 0.1°C/s. The sequences of all oligonucleotides used in this study were listed in Table S1.

Co-delivery of CRISPR components into human cells

Human 293T and Hep3B cells were seeded in 24-well plates at a density of 70,000∼100,000 cells per well for 24 h. For CRISPR-Cpf1 system, cells were treated with crRNA or its variants (500 ng [38 pmol] for *DNMT1* and *AAVS1* loci, and 1000 ng [76 pmol] for *FANCF* locus) formulated with Lipofectamine 3000 (Life Technologies) in Opti-MEM I reduced serum medium following the manufacturer's instructions. Meanwhile, Cpf1 plasmid (500 ng for *DNMT1* locus) or Ψ-modified Cpf1 mRNA (TriLink BioTechnologies, 500 ng for *DNMT1* and *AAVS1* loci, and 1000 ng for *FANCF* locus) were formulated with the same protocol and added to each well. Cells treated with the wild-type crRNA plus Cpf1 plasmid (or Cpf1 mRNA) served as the control group. Regarding RNP delivery, 5.85 μg [38 pmol] of AsCpf1 protein was incubated with equimolar chemically modified crRNA (500 ng [38 pmol], containing five 2′-fluoro ribose at the 3′ terminus) (Li et al., 2018a; Li et al., 2017) in Opti-MEM I reduced serum medium at 37°C for 10 min to form AsCpf1-crRNA RNP complexes. For CRISPR-Cas9 system, 100 ng of sgRNA and 1000 ng of Ψ-modified SpCas9 mRNA (TriLink BioTechnologies) were used. All components were delivered by Lipofectamine 3000.

Time- and dose-dependent inhibitory effects of PS-modified DNA oligonucleotides

In order to study the effects of time interval, 2.5 times molar excess of PS-modified DNA oligonucleotides over crRNA or sgRNA was formulated with Lipofectamine 3000, and added to cells co-delivered with the above described Cpf1 mRNA and Cpf1 crRNA or Cpf1 RNP at the indicated time points (0, 1, 3, 5 and 10 h). In the case of dose-dependence assay, Cpf1 mRNA- and crRNA-treated cells were exposed to different concentrations of PS-modified DNA oligonucleotides (the molar ratio of PS-DNA: crRNA ranged from 1: 6.25 to 6.25: 1) at 5 h. In both conditions, the end point was 48 h after the addition of CRISPR-Cpf1 components.

T7E1 enzymatic cleavage assays

Two days after treatment, genomic DNA was harvested from treated cells using the DNeasy Blood & Tissue Kit (QIAGEN). Polymerase chain reactions (PCRs) were then performed using Q5 Hot-start High-Fidelity DNA Polymerase (New England Biolabs). Primers (Eurofins Genomics) flanking the targeted region were listed in Table S2. The PCR products were annealed in NEBuffer 2 (50 mM NaCl, 10 mM Tris-HCl, 10 mM $MgCl_2$, 1 mM DTT, New England Biolabs) and subsequently digested by T7 Endonuclease I (T7E1, New England Biolabs) at 37°C for 30 min. The fraction cleaved was separated on 2% agarose gels, visualized on the ChemiDoc MP imaging system (Bio-Rad Laboratories), and analyzed by the Image Lab 5.2 analysis software (Bio-Rad Laboratories).

EMSAs

EMSAs were performed using 0.5 pmol of oligonucleotides and 0.25 pmol∼16 pmol of AsCpf1 protein (generously provided by New England Biolabs) at 37°C for 30 min in 7 uL of NEBuffer 3 (100 mM NaCl, 50 mM Tris-HCl, 10 mM $MgCl_2$, 1 mM DTT, New England Biolabs). The binding reactions were fractionated on 15% non-denaturing TBE polyacrylamide gels (Bio-Rad Laboratories), stained by SYBR Gold dye (Thermo Fisher Scientific), and detected on the ChemiDoc MP imaging system (Bio-Rad Laboratories).

Cpf1-mediated *in vitro* cleavage assays

To mimic human genomic cleavage, the target *DNMT1* locus was amplified from genomic DNA isolated from untreated 293T cells using Q5 High-Fidelity DNA Polymerase and primers listed in Table S2. PCR amplicons used as the DNA substrate were cleaned up with QIAquick PCR Purification Kit (QIAGEN). Prior to cleavage, crRNA (0.5 pmol) was equilibrated with different concentrations of AsCpf1 protein (crRNA: AsCpf1 protein is from 1: 1 to 1: 16) for 30 min at 37°C in 7 uL of NEBuffer 3 solution. Subsequently, 3 uL of PCR amplicons (0.5 pmol, in NEBuffer 3 solution) was incubated with the above complex at 37°C for 30 min. AsCpf1 protein in the reactions were degraded by adding 1 uL of proteinase K. Subsequently, the reactions were resolved on 2% agarose gels, visualized by EZ-Vision In-Gel staining, and imaged on the ChemiDoc MP imaging system.

Inhibition of Cpf1 cleavage activity *in vitro*

AsCpf1 protein, crRNA, and DNA substrate were incubated at 37°C for 30 min at the molar ratio of 1: 8: 1 (crRNA: AsCpf1 protein: DNA substrate). In a separate experiment, AsCpf1 protein and crRNA were pre-assembled into RNP at 37°C for 30 min, and then incubated with DNA substrate at 37°C for 30 min. In both cases, 2.5-fold molar excess of ps42DNA over crRNA was added to the reaction mixture at different time points (t = 0, 5, 10, 15, 20, 25 min). The remaining procedures were the same as described above.

Visualization of Cpf1 protein, crRNA, and DNA substrate

To assess the effects of fluorescence labeled crRNA on genome editing efficiency, Cy5-labeled crRNA (Cy5crRNA) was first evaluated in 293T cells as described above. To visualize crRNA in the protein-nucleic acid complexes, Cy5crRNA was complexed with AsCpf1 protein at 37°C for 30 min at a molar ratio of 1: 8, followed by incubation with an equivalent mole of DNA substrate relative to crRNA at 37°C for 30 min. The reaction mixture was digested with or without proteinase K prior to agarose gel electrophoresis, and the signals of reaction products were collected via a ChemiDoc MP imaging system under SYBR Green and Cy5 filters. To visualize AsCpf1 protein in the protein-nucleic acid complexes, crRNA, uDNA-crRNA or ps42DNA-crRNA was complexed with Cpf1 protein at 37°C for 30 min at a molar ratio of 1: 8, and incubated with an equivalent mole of DNA substrate relative to crRNA at 37°C for 30 min. The remaining procedures were the same as mentioned above, except that the agarose gel was further stained with Coomassie Blue and imaged using the ChemiDoc MP imaging system (Bio-Rad Laboratories). In a parallel assay, the pre-assembled RNP was incubated with an equivalent mole of DNA substrate and 2.5-fold excess of PS-modified DNA relative to crRNA. The uncleaved DNA substrate was quantified by densitometric analysis and normalized to that of the untreated DNA substrate.

QUANTIFICATION AND STATISTICAL ANALYSIS

Histograms were generated using Prism software (GraphPad). Quantitative data in Figures 1C, 1E, 1F, 2B-2G, 3 and 5B are presented as the mean and standard deviation from three biological replicates. Statistical significance were evaluated using two-tailed Student's t test for comparisons between two groups. A p value of less than 0.05 (*, $p < 0.05$; **, $p < 0.01$; ***, $p < 0.001$) was considered statistically significant.

Cell Reports, Volume *25*

Supplemental Information

Synthetic Oligonucleotides Inhibit CRISPR-Cpf1-Mediated Genome Editing

Bin Li, Chunxi Zeng, Wenqing Li, Xinfu Zhang, Xiao Luo, Weiyu Zhao, Chengxiang Zhang, and Yizhou Dong

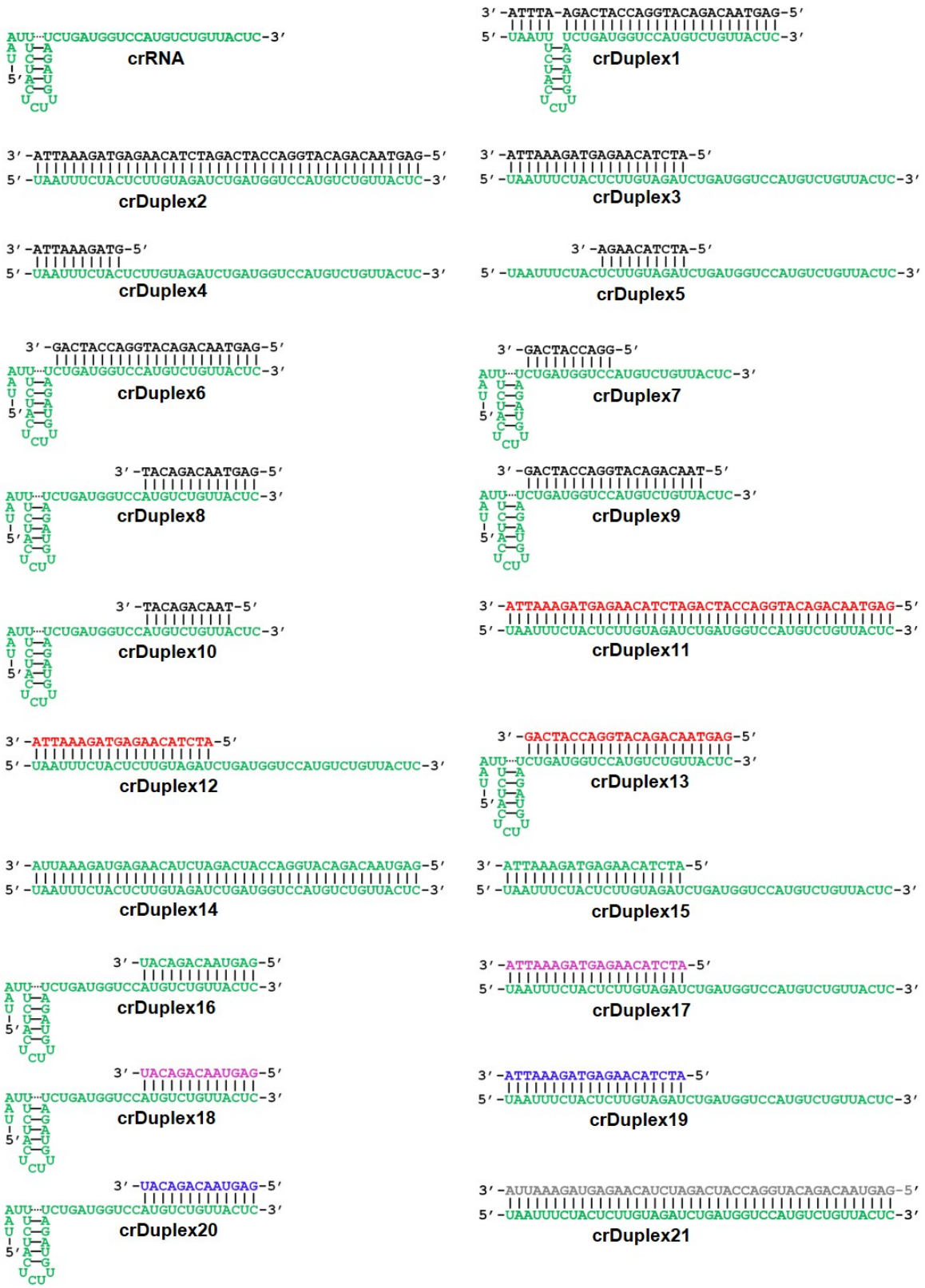

Figure S1. Structures of wild-type crRNA and crRNA duplexes. Related to Figure 1.

The green letter denotes the unmodified RNA nucleotide. The black letter denotes unmodified DNA nucleotide. The red letter denotes PS-linkage modified DNA. The violet letter denotes 2'-fluoro modified RNA. The blue letter denotes 2'-*O*-methyl modified RNA. The gray letter denotes PS-linkage modified RNA. Vertical lines represent complementary binding between paired bases.

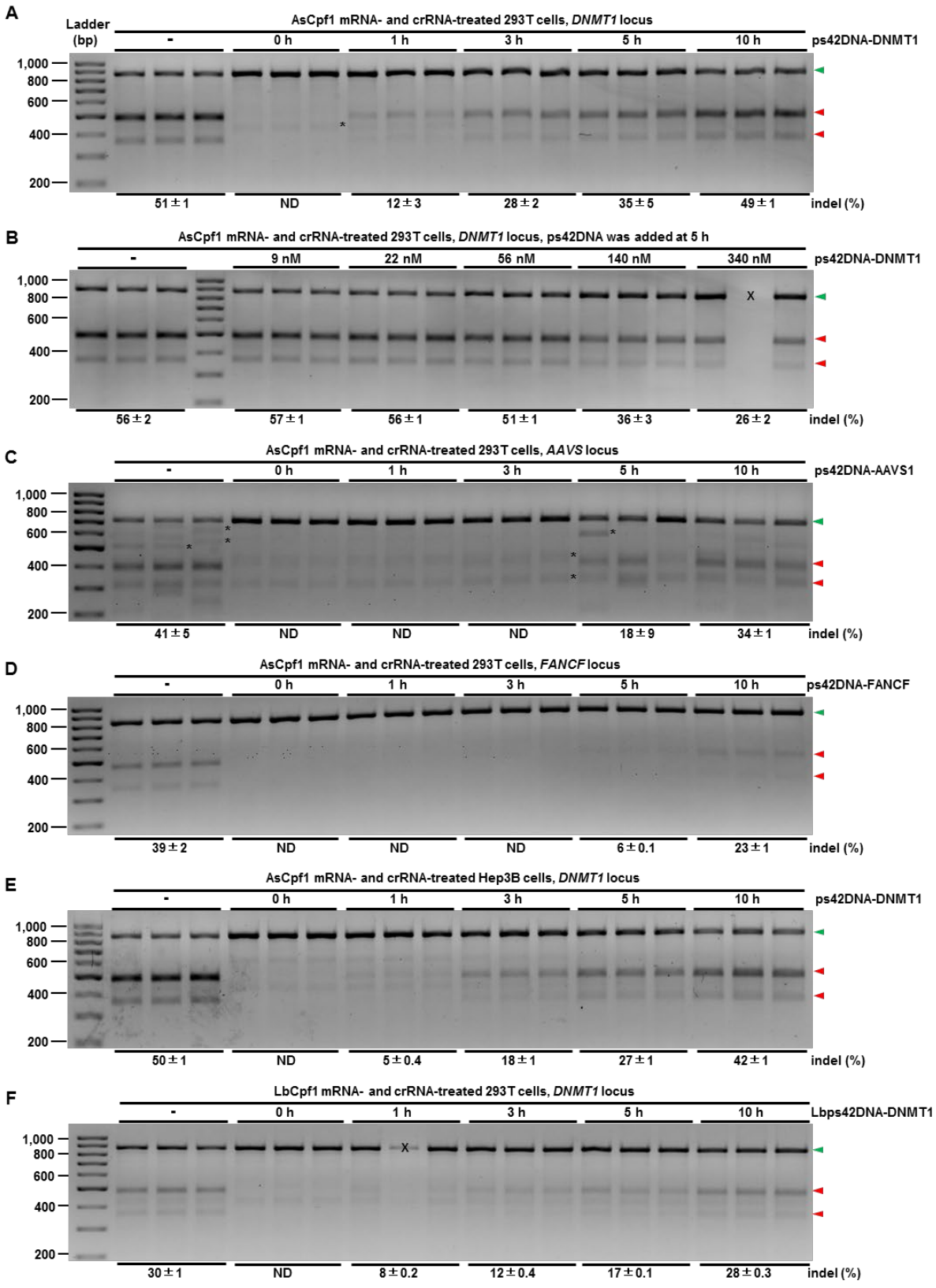

Figure S2. Inhibition effects of phosphorothioated DNA oligonucleotides on Cpf1-mediated genome editing in mammalian cells. Related to Figure 2.

(A) Time-dependent inhibitory effects of ps42DNA-DNMT1 on AsCpf1-mediated genome editing at the *DNMT1* locus in 293T cells. ps42DNA-DNMT1 was added at various time points after treatment with AsCpf1 mRNA and

crRNA targeting *DNMT1* locus. Related to Figure 2B.

(B) Dose-dependent inhibitory effects of ps42DNA on AsCpf1-mediated genome editing at the *DNMT1* locus in 293T cells. ps42DNA-DNMT1 was added at 5 h after treatment with CRISPR-Cpf1 mRNA and crRNA targeting *DNMT1* locus. Related to Figure 2C.

(C) Time-dependent inhibitory effects of ps42DNA-AAVS1 on AsCpf1-mediated genome editing at the *AAVS1* locus in 293T cells. ps42DNA-AAVS1 was added at various time points after treatment with AsCpf1 mRNA and crRNA targeting *AAVS1* locus. Related to Figure 2D.

(D) Time-dependent inhibitory effects of ps42DNA-FANCF on AsCpf1-mediated genome editing at the *FANCF* locus in 293T cells. ps42DNA-FANCF was added at various time points after treatment with AsCpf1 mRNA and crRNA targeting *FANCF* locus. Related to Figure 2E.

(E) Time-dependent inhibitory effects of ps42DNA on AsCpf1-mediated genome editing at the *DNMT1* locus in Hep3B cells. ps42DNA-DNMT1 was added at various time points after treatment with AsCpf1 mRNA and crRNA targeting *DNMT1* locus. Related to Figure 2F.

(F) Time-dependent inhibitory effects of Lbps42DNA-DNMT1 on LbCpf1-mediated genome editing at the *DNMT1* locus in 293T cells. Lbps42DNA-DNMT1 was added at various time points after treatment with LbCpf1 mRNA and LbCpf1 crRNA targeting *DNMT1* locus. Related to Figure 2G.

The control group (-) was treated only with AsCpf1 mRNA and crRNA. The concentration of inhibitors in (B) and (D)–(G) is 140 nM (2.5-fold molar excess relative to crRNA). Relative genome-editing efficiency in (B)–(G) was determined using the T7E1 cleavage assay from three biological replicates 48 hr post-treatment. The lane marked with "×" is excluded for calculation of genome editing efficiency. The time points above gels denote the time to add inhibitors, and the asterisks denote the non-specific bands. The green and red arrowheads denote the intact DNA substrate and cleaved DNA fragments, respectively.

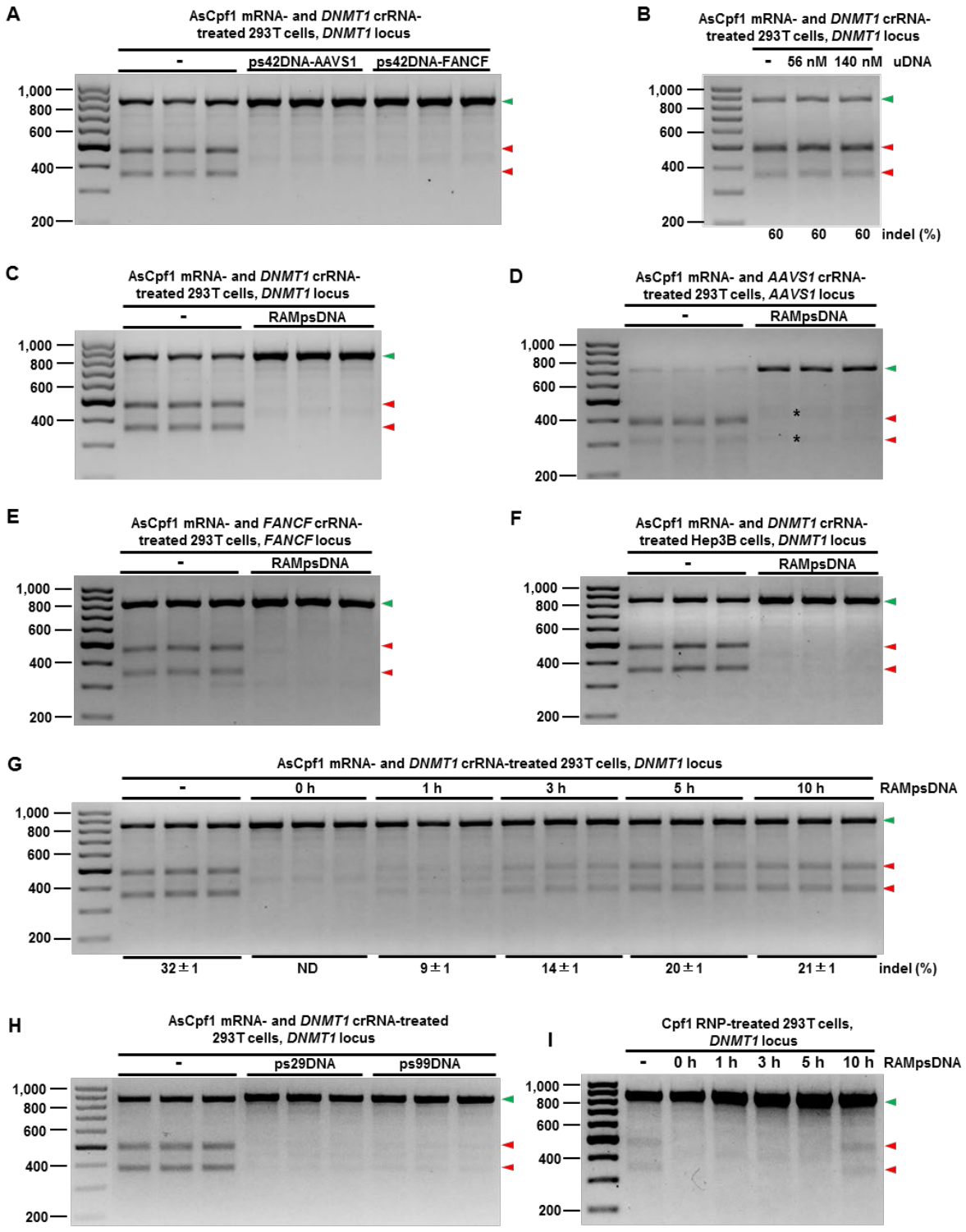

Figure S3. Inhibitory effects of RAMpsDNA against Cpf1 in human cells. Related to Figure 3.

(A) Inhibitory effects of ps42DNA-AAVS1 and ps42DNA-FANCF on AsCpf1-mediated genome editing at the *DNMT1* locus in 293T cells. ps42DNA-AAVS1 or ps42DNA-FANCF was added simultaneously with AsCpf1 mRNA and AsCpf1 crRNA targeting *DNMT1* locus. Related to Figure 3A.

(B) A representative gel image for assessment of the impact of uDNA on AsCpf1-mediated genome editing at the *DNMT1* locus in 293T cells. uDNA was added at 0 h after treatment with CRISPR-Cpf1 mRNA and crRNA targeting the *DNMT1* locus.

(C) Inhibitory effects of RAMpsDNA on AsCpf1-mediated genome editing at the *DNMT1* locus in 293T cells. RAMpsDNA was added simultaneously with CRISPR-Cpf1 mRNA and crRNA targeting the *DNMT1* locus. Related to Figure 3B.

(D) Inhibitory effects of RAMpsDNA on AsCpf1-mediated genome editing at the *AAVS1* locus in 293T cells. RAMpsDNA was added simultaneously with CRISPR-Cpf1 mRNA and crRNA targeting the *AAVS1* locus. Related to Figure 3B.

(E) Inhibitory effects of RAMpsDNA on AsCpf1-mediated genome editing at the *FANCF* locus in 293T cells. RAMpsDNA was added simultaneously with CRISPR-Cpf1 mRNA and crRNA targeting the *FANCF* locus. Related to Figure 3B.

(F) Inhibitory activity of RAMpsDNA on AsCpf1-mediated genome editing at the *DNMT1* locus in Hep3B cells. RAMpsDNA was added simultaneously with CRISPR-Cpf1 mRNA and crRNA targeting *DNMT1* locus. Related to Figure 3C.

(G) Time-dependent inhibitory effects of RAMpsDNA on AsCpf1-mediated genome editing at the *DNMT1* locus in 293T cells. The time points above gels denote the time to add RAMpsDNA. Genome editing efficiency was determined by the T7E1 cleavage assay three biological replicates. Related to Figure 3D.

(H) The effects of RAMpsDNA length on on AsCpf1-mediated genome editing at the *DNMT1* locus in 293T cells. Phosphorothioated DNA oligonucleotides with different length was added simultaneously with CRISPR-Cpf1 mRNA and crRNA targeting *DNMT1* locus.

(I) Inhibitory activity of RAMpsDNA on Cpf1-RNP mediated genome editing at the *DNMT1* locus in 293T cells. RAMpsDNA was added at various time points after treatment with AsCpf1 mRNA and crRNA targeting *DNMT1* locus.

The control group (-) was treated only with AsCpf1 mRNA and crRNA or Cpf1 RNP. The concentration of inhibitors in (A) and (C)-(I) is 140 nM (2.5-fold molar excess relative to crRNA). T7E1 cleavage assays were conducted 48 hr post-treatment. The asterisks denote the non-specific bands. The green and red arrowheads denote the intact DNA substrate and cleaved DNA fragments, respectively.

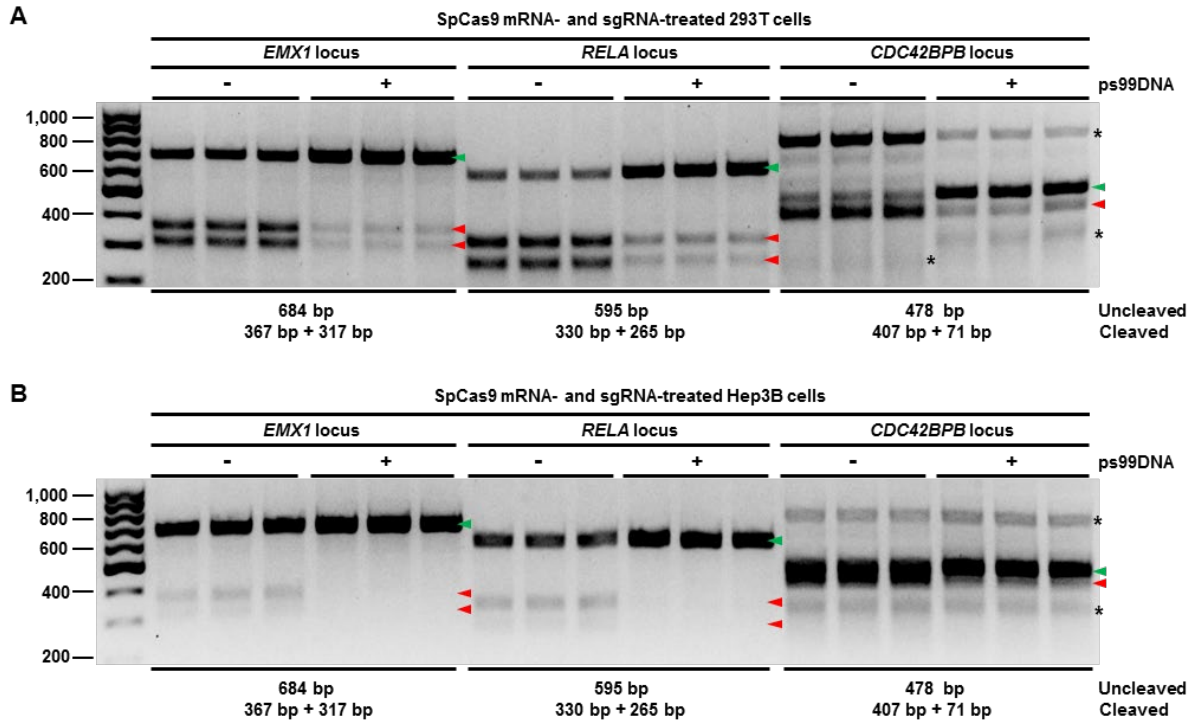

Figure S4. Inhibitory effects of phosphorothioated DNA oligonucleotides on Cas9-mediated genome editing in mammalian cells. Related to STAR Methods.

(A) Inhibitory effects of ps99DNA on SpCas9-mediated genome editing at the *EMX1*, *RELA*, and *CDC42BPB* loci in 293T cells. ps99DNA was added simultaneously with CRISPR-Cas9 mRNA and sgRNA targeting the *EMX1*, *RELA*, or *CDC42BPB* loci.

(B) Inhibitory effects of ps99DNA on SpCas9-mediated genome editing at the *EMX1*, *RELA*, and *CDC42BPB* loci in Hep3B cells. ps99DNA was added simultaneously with CRISPR-Cas9 mRNA and sgRNA targeting the *EMX1*, *RELA*, or *CDC42BPB* loci.

The control group (-) was treated only with SpCas9 mRNA and sgRNA. T7E1 cleavage assays were conducted 48 hr post-treatment. Asterisks denote the non-specific bands. The green and red arrowheads denote the intact DNA substrate and cleaved DNA fragments, respectively.

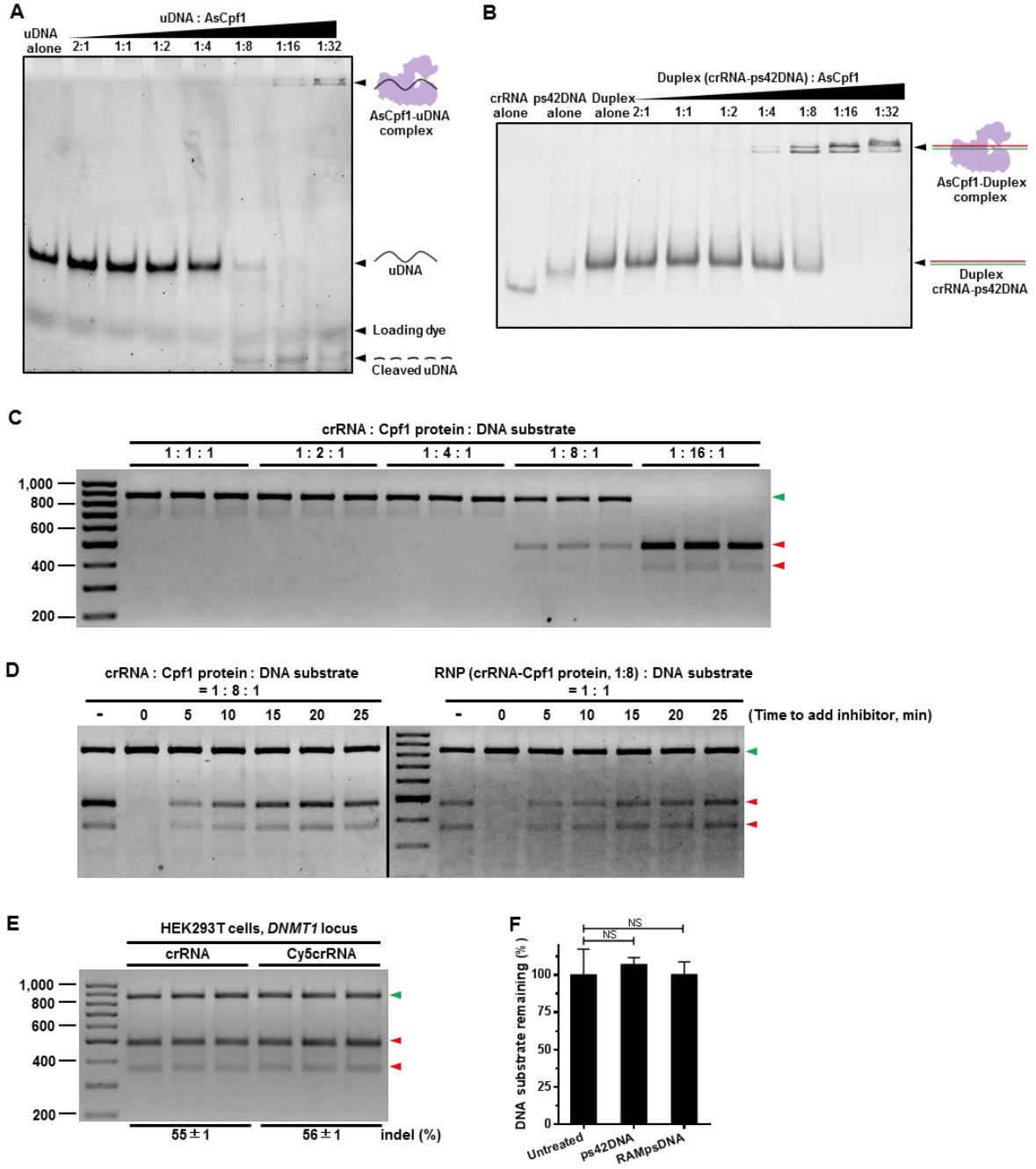

Figure S5. Cpf1-mediated *in vitro* cleavage assay. Related to Figure 4 and Figure 5.

(A) AsCpf1 protein-induced unmodified DNA (uDNA) cleavage in the absence of crRNA.

(B) Interactions between AsCpf1 protein and duplex crRNA-ps42DNA.

(C) AsCpf1-mediated DNA cleavage in vitro in the presence of wild-type crRNA at the indicated molar ratio of crRNA : AsCpf1 protein: DNA substrate. The reaction mixtures were treated with proteinase K to release the short cleaved fragment complexed with AsCpf1 protein.

(D) The time course of the inhibitory effect of ps42DNA. Left, three components including crRNA, AsCpf1 protein, and the target DNA substrate were incubated at 37°C for 30 min. Right, crRNA and AsCpf1 protein were pre-assembled into RNP at 37°C for 30 min, and then incubated with the target DNA substrate at 37°C for 30 min. In both panels. The inhibitor ps42DNA was added to the reaction at the indicated time points. The vertical line

indicates the border between two separate gels.
(E) Comparison of genome editing efficiency of crRNA and Cy5crRNA at the *DNMT1* locus in the presence of AsCpf1 plasmid in 293T cells. Genome editing efficiency (%) was determined by the T7E1 cleavage assay 48 h post-transfection.
(F) Quantification of DNA substrate remaining (%) in the presence of AsCpf1 protein, crRNA and ps42DNA (or RAMpsDNA). The uncleaved DNA substrate was quantified by densitometric analysis and normalized to the DNA substrate alone group. Data are expressed as the mean ± SD from three biological replicates (NS, not significant; two-tailed t-test).
Gels in (A) and (B) were resolved on 15% non-denaturing TBE polyacrylamide gels and stained by SYBR Gold. Gels in (C)-(E) were separated on 2% agarose gels and stained by EZ-Vision In-Gel staining. The green and red arrowheads denote the intact DNA substrate and cleaved DNA fragments, respectively.

Table S1. crRNAs and oligonucleotides used in this study. Related to Figures 1-5.

Oligonucleotides	**Length (nt)**	**Sequence (5' to 3')**
AsCpf1 crRNA targeting *DNMT1*	43	UAAUUUCUACUCUUGUAGAUCUGAUGGUCCAUGUCUG UUACUC
Oligo 1	29	GAGTAACAGACATGGACCATCAGAAATTA
Oligo 2 (uDNA)	43	GAGTAACAGACATGGACCATCAGATCTACAAGAGTAGA AATTA
Oligo 3	20	ATCTACAAGAGTAGAAATTA
Oligo 4	10	GTAGAAATTA
Oligo 5	10	ATCTACAAGA
Oligo 6	23	GAGTAACAGACATGGACCATCAG
Oligo 7	10	GGACCATCAG
Oligo 8	13	GAGTAACAGACAT
Oligo 9	20	TAACAGACATGGACCATCAG
Oligo 10	10	TAACAGACAT
Oligo 11 (ps42DNA-DNMT1)	43	GAGTAACAGACATGGACCATCAGATCTACAAGAGTAGA AATTA
Oligo 12	20	ATCTACAAGAGTAGAAATTA
Oligo 13	23	GAGTAACAGACATGGACCATCAG
Oligo 14	43	GAGUAACAGACAUGGACCAUCAGAUCUACAAGAGUAG AAAUUA
Oligo 15	20	AUCUACAAGAGUAGAAAUUA
Oligo 16	13	GAGUAACAGACAU
Oligo 17	20	AUCUACAAGAGUAGAAAUUA
Oligo 18	13	GAGUAACAGACAU
Oligo 19	20	AUCUACAAGAGUAGAAAUUA
Oligo 20	13	GAGUAACAGACAU
Oligo 21	13	GAGUAACAGACAUGGACCAUCAGAUCUACAAGAGUAG AAAUUA
Randomized ps42DNA (RAMpsDNA)	43	AGACGTACAGTAAGACAATAAGACCGAACTTAGCATAT GGAAT
Randomized ps29DNA	30	AGACGTACAGTAAGACAATAAGACCGAACT
AsCpf1 crRNA targeting *AAVS*	43	UAAUUUCUACUCUUGUAGAUCUUACGAUGGAGCCAGA GAGGAU
ps42DNA-AAVS1	43	ATCCTCTCTGGCTCCATCGTAAGATCTACAAGAGTAGAA ATTA
AsCpf1 crRNA targeting *FANCF*	43	UAAUUUCUACUCUUGUAGAUGUCGGCAUGGCCCCAUU CGCACG
ps42DNA-FANCF	43	CGTGCGAATGGGGCCATGCCGACATCTACAAGAGTAGA AATTA
LbCpf1 crRNA targeting *DNMT1*	43	AAUUUCUACUAAGUGUAGAUCUGAUGGUCCAUGUCUG UUACUC
Lbps42DNA-DNMT1	43	GAGTAACAGACATGGACCATCAGATCTACAAGAGTAGA

		AATTA
SpCas9 sgRNA targeting *EMX1*	100	GAGUCCGAGCAGAAGAAGAA + scaffold
ps99DNA	100	Reversely complement of scaffold + TTCTTCTTCTGCTCGGACTC
SpCas9 sgRNA targeting *RELA*	100	GAUCUCCACAUAGGGGCCAG + scaffold
SpCas9 sgRNA targeting *CDC42BPB*	100	GAGCCGCACCUUGGCCGACA + scaffold

Unmodified RNA nucleotides are shown in green. Unmodified DNA nucleotides are shown in black. PS-linkage modified DNA nucleotides are shown in red. 2'-fluoro modified RNA nucleotides are shown in violet. 2'-*O*-methyl modified RNA nucleotides are shown in blue. PS-linkage modified RNA nucleotides are shown in gray.

Table S2. A list of primers used for T7E1 assay and *in vitro* cleavage reaction. Related to Figures 1-3, and 5.

Locus	Forward primer	Reverse primer
DNMT1	CTGGGACTCAGGCGGGTCAC	CCTCAGCCAGAAGTCCCGTGC
AAVS1	GGGCTGGCTACTGGCCTTAT	ATGGCATCTTCCAGGGGTCC
FANCF	AGCTCCGCCTGGGTCTTCAT	GCGGAGACGTTCATGACTGG
EMX1	AAAACCACCCTTCTCTCTGGC	GGAGATTGGAGACACGGAGAG
RELA	TTCTAGGGAGCAGGTCCTGACT	TCCTTTCCTACAAGCTCGTGGG
CDC42BPB	GCGCCCTGACGGACTGGCCGA	GGAGGGCAAGGAGGGATGAAAA